

Distinct Mechanisms of Agonist-induced Endocytosis for Human Chemokine Receptors CCR5 and CXCR4

Sundararajan Venkatesan,^{*†} Jeremy J. Rose,^{*‡} Robert Lodge,^{‡§}
Philip M. Murphy,[¶] and John F. Foley[#]

^{*}Laboratory of Molecular Microbiology, [¶]Laboratory of Host Defenses and [#]Laboratory of Clinical Investigation, National Institute of Allergy and Infectious Diseases, and [‡]Cell Biology and Metabolism Branch, National Institute of Child Health and Human Development, National Institutes of Health, Bethesda, Maryland 20892

Submitted November 6, 2002; Revised April 1, 2003; Accepted April 4, 2003
Monitoring Editor: Suzanne Pfeffer

Desensitization of the chemokine receptors, a large class of G protein-coupled receptors, is mediated in part by agonist-driven receptor endocytosis. However, the exact pathways have not been fully defined. Here we demonstrate that the rate of ligand-induced endocytosis of CCR5 in leukocytes and expression systems is significantly slower than that of CXCR4 and requires prolonged agonist treatment, suggesting that these two receptors use distinct mechanisms. We show that the C-terminal domain of CCR5 is the determinant of its slow endocytosis phenotype. When the C-tail of CXCR4 was exchanged for that of CCR5, the resulting CXCR4-CCR5 (X4-R5) chimera displayed a CCR5-like trafficking phenotype. We found that the palmitoylated cysteine residues in this domain anchor CCR5 to plasma membrane rafts. CXCR4 and a C-terminally truncated CCR5 mutant (CCR5-KRFX) lacking these cysteines are not raft associated and are endocytosed by a clathrin-dependent pathway. Genetic inhibition of clathrin-mediated endocytosis demonstrated that a significant fraction of ligand-occupied CCR5 trafficked by clathrin-independent routes into caveolin-containing vesicular structures. Thus, the palmitoylated C-tail of CCR5 is the major determinant of its raft association and endocytic itineraries, differentiating it from CXCR4 and other chemokine receptors. This novel feature of CCR5 may modulate its signaling potential and could explain its preferential use by HIV for person-to-person transmission of disease.

Article published online ahead of print. Mol. Biol. Cell 10.1091/mbc.E02-11-0714. Article and publication date are available at www.molbiolcell.org/cgi/doi/10.1091/mbc.E02-11-0714.

[†] Corresponding author. E-mail address: aradhana@helix.nih.gov or sv1s@nih.gov.

[§] Present address: INRS-Institut Armand-Frappier, Université du Québec, 531 des Prairies, Laval (Québec), Canada H7V 1B7. Abbreviations used: AOP-RANTES, aminooxypentane-regulated on activation, normal T-cell expressed and secreted; APC, allophycocyanin; Arf6, ADP-ribosylation factor 6; CCV, clathrin-coated vesicles; CHO, Chinese hamster ovary; CKRs, chemokine receptors; CTx-B, B subunit of cholera toxin; C-terminal, carboxy-terminal; C-tail, carboxy-terminal tail; DRMs, detergent resistant membranes; EGFR, epidermal growth factor receptor; FITC, fluorescein isothiocyanate conjugated; GPCRs, G protein-coupled receptors; GPI, glycosyl phosphatidylinositol; GRKs, G protein-coupled receptor kinases; HEK, human embryonic kidney; IL-2 or IL-8, interleukin-2 or -8; LDL, low-density lipoprotein; MFV, mean fluorescence value; MHC-I, class I major histocompatibility; MIP, macrophage inflammatory protein; M-tropic, macrophage tropic; N-terminal, amino-terminal; PBL, peripheral blood lymphocyte; PE, phycoerythrin; PFA, paraformaldehyde; RT, room temperature; SDF, stromal derived factor; Tfn, transferrin; Tfn-R, transferrin receptor; TM, transmembrane; TR, Texas Red; T-tropic, T-cell tropic; wt, wild-type.

INTRODUCTION

Clathrin-mediated endocytosis has been the general paradigm and the most extensively studied mechanism of ligand-induced receptor internalization (Schmid, 1997). However, in recent years, alternative clathrin-independent mechanisms have been described for the uptake of viruses, toxins, and receptors that lack conventional endocytic signals (Nichols and Lippincott-Schwartz, 2001). Among the latter mechanisms, cholesterol-rich structures called caveolae (Anderson, 1998; Kurzchalia and Parton, 1999) and lipid rafts (Nichols *et al.*, 2001) have been implicated in diverse membrane processes including the assembly of signaling receptor complexes (Simons and Toomre, 2000). Endocytosis of some receptors such as the α subunit of the IL-2 receptor (Tac antigen) and MHC-I, which lack canonical endocytic signals, follow distinct itineraries regulated by the small GTP binding protein, ADP-ribosylation factor 6 (Arf6; Radhakrishna and Donaldson, 1997; Sugita *et al.*, 1999). Clathrin-independent endocytic itineraries are slower than the clathrin-dependent pathway and are functionally relevant in that the long residence time of occupied receptors at the cell surface may enable coupling to multiple signaling pathways.

CKRs are a specialized subset of GPCRs that mainly regulate leukocyte migration but also have effects on development and other processes (Sallusto *et al.*, 2000). The receptors are broadly grouped into CC, CXC, CX3C, and C classes, based on the structure of their cognate agonists (Murphy *et al.*, 2000). The ability of CKRs to sense an agonist gradient during chemotaxis is governed by three distinct mechanisms: desensitization, internalization, and recovery. CKR desensitization occurs within seconds of activation and is mediated by phosphorylation of the receptor by a G protein-coupled receptor kinase (GRK) followed by recruitment of β -arrestin, which uncouples the CKR from G protein activation (Ferguson *et al.*, 1998; Krupnick and Benovic, 1998). The interactions of β -arrestin with clathrin and the $\beta 2$ subunit of the AP-2 adapter complex (Krupnick *et al.*, 1997; Laporte *et al.*, 1999) facilitate the recruitment of the CKRs into endocytic vesicles.

Among the CKRs, CCR5 and CXCR4 have been the subjects of intense study, particularly because of their function as coreceptors for M and T-tropic HIV, respectively (Berger *et al.*, 1999). Following the discovery that HIV infection was inhibited by treatment with chemokines specific for CCR5 or CXCR4 (Cocchi *et al.*, 1995; Bleul *et al.*, 1996; Oberlin *et al.*, 1996), receptor agonists or antagonists have been used to block HIV infection by promoting receptor internalization or by steric hindrance (Amara *et al.*, 1997; Simmons *et al.*, 1997). In both primary lymphocytes and expression systems, CCR5 has been reported to internalize upon binding agonists. In CHO cells, internalized CCR5 has been reported to colocalize in endosomes with transferrin receptor (Tfn-R), which was used to label the clathrin pathway (Mack *et al.*, 1998). Likewise, agonist occupied CXCR4 underwent clathrin-dependent endocytosis in both primary cells and ectopic expression systems (Amara *et al.*, 1997). Although these studies implied that agonist-driven endocytosis of CCR5 followed the clathrin pathway, a recent report suggested that CCR5 endocytosis followed both clathrin- and caveolae-dependent routes in CHO and HeLa cells (Mueller *et al.*, 2002).

Although previous studies (Amara *et al.*, 1997; Mack *et al.*, 1998) examined the rate and route of CCR5 and CXCR4 internalization in both T cells and stable cell lines, there has not been a quantitative head-to-head comparison of the two. Moreover, their localization to specific plasma membrane domains has not been clearly defined. We have carried out a comparative study to clarify the trafficking itineraries of CCR5 and CXCR4 and addressed the structural elements of the receptors that determine their internalization routes. In particular, we focused on the C-tail of CCR5 that contains a bipartite motif composed of a basic domain followed by a cysteine cluster that is critical for optimal anterograde transport and cell surface expression (Venkatesan *et al.*, 2001). Palmitoylation of the cysteine cluster is crucial for optimal plasma membrane insertion (Blanpain *et al.*, 2001; Kraft *et al.*, 2001; Percherancier *et al.*, 2001). Now we show that the C-terminal domain, and particularly the cysteine residues, couple CCR5 to additional clathrin-independent pathways, which may include caveolin participation, and are dependent on the selective partitioning of the receptor to cholesterol-enriched raft microdomains.

MATERIALS AND METHODS

Expression Plasmids, Cell Lines, and Cell Transfection

Expression plasmids for all wt CKRs and their mutants and chimeras have been described (Venkatesan *et al.*, 2001). HA-tagged wt caveolin-3 and N-terminal CAV^{DGV} or CAV^{KSY} mutant plasmids were from John Hancock of the University of Queensland, Australia (Roy *et al.*, 1999). Eps15 deletion mutant fused amino-terminally to GFP (GFP-E Δ 95/295) was obtained from Alexandre Benmerah (INSERM, Paris, France; Benmerah *et al.*, 1999). YFP fusion proteins of wt and mutant forms of rab5 GTPase have been previously described (Nichols *et al.*, 2001). FLAG epitope-tagged C-terminal fragment of AP180 was obtained from Julie Donaldson and Lois Greene of LCB, NICHD, NIH. Expression plasmid for caveolin1-GFP fusion protein (Volonte *et al.*, 1999) was obtained from Lois Greene of LCB, NICHD. PBLs were isolated from whole blood, buffy coat or lymphocyte rich leukopaks provided by the Department of Transfusion Medicine at the Clinical Center, NIH. RBCs were disrupted with ACK lysis solution and removed by gentle centrifugation. The final pellet of PBMCs was suspended in RPMI with 10% FCS. For T-cell activation, PBMCs purified by banding after FICOLL-HYPAQUE centrifugation were stimulated by CD3 mAb for 36 h in the presence of IL-2 (20 IU/ml) in RPMI with 10% FCS, following which they were propagated in medium containing IL-2. HOS cells stably expressing CD4 and CCR5, CXCR4 or CCR3 were from the AIDS Reference and Reagent Program, DAIDS, NIAID, NIH. HEK293 cells stably expressing CCR5, CXCR1, or CXCR2 have been described (Alkhatib *et al.*, 1997). Cells were transfected by using Fugene (Roche Diagnostics, Piscataway, NJ) or polyfectin (Qiagen Inc., Valencia, CA) reagents according to manufacturer's instructions. For FACS analysis experiments, CD4 or CD8 was coexpressed to control for variation. For microscopy, DNA transfection was carried out on cells plated on glass coverslips in 24-well plates or on Nunc Titer-Tek (Nalge Nunc International, Rochester, NY) cover glass chambers.

Antibody Binding and Flow Cytometric Analysis

Dye-conjugated or unconjugated mAbs or rabbit antisera against various CKRs, CD4, CD8, CD3, CD45, CD71 were obtained either from commercial sources (Becton Dickinson Immunocytometry Division, Caltag Corp., R & D Systems, or Zymed Labs, South San Francisco, CA) or gifted by the NIH AIDS Reference and Reagent Program. Rabbit IgG raised against the N-terminal peptide of CCR5 has been described before (Venkatesan *et al.*, 2001). Rabbit anti-serum against an analogous epitope of CXCR4 was donated by Chris Broder of USUHS (Bethesda MD). Zymed Corp. was the source for rabbit IgG against human Tfn-R. Mouse monoclonal antibodies and rabbit antisera against various caveolin isoforms were from PharMingen Division of Becton Dickinson (San Diego, CA) and Santa Cruz Biotechnology Inc. (Santa Cruz, CA). Dye- or biotin-conjugated and unlabeled 12CA5 mAb against the HA epitope was from Roche Diagnostic/Boehringer Mannheim Corp. (Indianapolis, IN). Murine monoclonal antibodies and rabbit IgG against FLAG epitope was from Sigma-Aldrich, Inc. (St. Louis, MO). For secondary staining, dye-conjugated purified Fab fragments with the relevant species-specific reactivity were obtained from commercial sources (Molecular Probes, Eugene, OR) and Jackson ImmunoResearch Lab (West Grove, PA). Dye-conjugated Tfn, LDL, 10K dextran, and CTX-B were from Molecular Probes.

Cell surface receptor density was quantified by FACS analysis (Venkatesan *et al.*, 2001). Typically, 10^5 cells were incubated for 15 min at 25°C with the appropriate antibodies in 0.1 ml of PBS containing 1% BSA or 1% FCS and 0.02% sodium azide. Flow cytometric data acquisition was carried out using a dual laser four-color Becton Dickinson FACSort flow cytometer. Data analysis was done using CELLQUEST v3.3 (BD-PharMingen) and FlowJo v3.3.4 (Tree Star Inc., San Carlos, CA) software.

Steady State and Kinetic Evaluation of Receptor Internalization and Recycling

Chemokines were purchased from Peprtech Inc. (Rocky Hill, NJ), except for AOP-RANTES, which was from Gryphon Sciences Inc. (South San Francisco, CA). For receptor internalization assay by FACS, cells were starved in serum-free medium for 20 min. Cells, 10^6 , were then incubated in RPMI containing 1% BSA and challenged with the appropriate agonists at different concentrations for the indicated times. Cells were rinsed several times and incubated with fluorochrome-conjugated mAbs and processed for FACS analysis as described above. For kinetics analysis, chemokine concentrations were optimized to induce 50% receptor loss on the cell surface after a 30-min incubation. For receptor recycling experiments, cell lines expressing the indicated receptor(s) were treated for 30 min with cycloheximide and anisomycin (each at 25 $\mu\text{g}/\text{ml}$) before and during the course of the experiment. Under these conditions, incorporation of [^{35}S]methionine into proteins was arrested >99%. Agonist stimulation was for 30 min at 37°C in DMEM containing 1% BSA with AOP-RANTES at 100 nM and all other agonists at 50 nM. After stimulation, cells were rinsed in DMEM, maintained in growth medium with protein synthesis inhibitors, and periodically monitored by FACS analysis.

Microscopic Visualization of Receptor Internalization

We compared the retrograde trafficking of agonist stimulated CKRs with that of ligand-bound Tfn-R. HOS or HEK 293 cells stably expressing the indicated receptors, HeLa CD4 clones overexpressing CXCR4, or HeLa cells transiently expressing the various receptors were used. Cells on coverslips at 50% confluence were starved for 30 min at 37°C in DMEM without serum. They were then incubated at 37°C for 30 min in 200 μl DMEM (with 0.5% BSA) with fluorochrome-conjugated Tfn (50 $\mu\text{g}/\text{ml}$) and in the presence or absence of the respective chemokines. CXCR4 cells were also treated with phorbol-12,13-dibutyrate (PdBu). Cells were rinsed three times at the end of incubation, fixed in PFA, permeabilized by 10-min treatment at RT with 0.25% Triton X-100 in PBS, and stained with dye-conjugated mAbs against the respective CKRs. Cells were then rinsed and mounted in Fluoromount-G (Southern Biotechnology Associates, Birmingham, AL).

Although the above procedure worked well in stable cell lines with receptors undergoing rapid transit, in some continuous cell lines and transient transfectants, not all the de novo synthesized receptor(s) was expressed at the cell surface. As such, it was sometimes difficult to discriminate receptors in intracellular vesicles as resulting from endocytosis rather than reflecting intracellular stasis due to slow or aberrant anterograde transport. This was generally not problematic with CXCR4 and other CXC receptors that exhibited brisk retrograde trafficking upon agonist treatment and had no serious delays in the biosynthetic itinerary. Therefore, we monitored the internalization of receptor-bound antibodies. For agonist-driven receptor internalization assay, starved cells were incubated at RT for 30–60 s with the respective chemokine- and dye-conjugated Tfn (50 $\mu\text{g}/\text{ml}$); dye-conjugated receptor mAb (10 μl mAbs or 1–2 μg equivalent) was then added, and incubation continued for indicated times. In some experiments, antibodies and Tfn were bound at 4°C for 15 min, before agonist treatment. At the concentrations used, the mAbs did not interfere with signaling from the respective receptors. Cells were then rinsed several times in PBS, fixed in 4% PFA, rinsed again, and mounted for microscopy. In some experiments (indicated in the relevant figure legends), cell surface-bound antibody was stripped by treatment for 1 min with 0.5% acetic acid in 500 mM NaCl. Although this procedure was generally effective in eluting dye-conjugated primary antibodies, the elution of unconjugated antibodies was incomplete. When the cells were reacted with unconjugated 1° antibodies followed by acid wash before staining with dye-labeled 2° antibodies, a fair amount

of residual cell surface-bound antibody (rabbit IgG being worse than murine mAb) was present.

Methyl β -cyclodextrin, Fillipin Treatments and Cholesterol Repletion, and Triton X-100 Extraction

Methyl β -cyclodextrin (Trappsol grade) was from CT Inc. (High Springs, FL). Cells were suspended in medium without serum and treated with various concentrations of cyclodextrin (CyDx) for 30 min at 37°C. They were then rinsed and incubated in growth medium with 1% lipid-free BSA (Sigma-Aldrich Corp.) or delipidated serum. In some cases, CyDx treatment was continued during the experiment. The efficiency of cholesterol extraction was checked microscopically by fillipin (10 $\mu\text{g}/\text{ml}$) staining. Cells plated on coverslips were treated with cyclodextrin or left untreated, fixed in 4% PFA, and rinsed in PBS before fillipin staining. For cholesterol depletion by fillipin extraction, cells were incubated in PBS with increasing amounts of fillipin to determine cell viability, and at ≈ 50 $\mu\text{g}/\text{ml}$, most monolayers exhibited severe morphological changes. In general, fillipin treatment at ~ 10 $\mu\text{g}/\text{ml}$ induced losses in cell surface CCR5 that were comparable with cyclodextrin treatment at 5 mM. For FACS analysis, monolayers on six-well plates were dislodged by a 10-min treatment at 37°C with 5 mM EDTA in PBS and processed as described above. For microscopy, cells plated on glass coverslips were stained with the indicated antibodies. Cholesterol feeding was done by incubating cells at 37°C for 30 min in PBS with 300 μM cholesterol and 150 mM CyDx. Triton X-100 extraction was carried out with cells plated on coverslips. Two different protocols of detergent extraction were used. In the SFT (Stain, Fix, Triton X-100 treat) protocol, monolayers on coverslips were stained with the respective antibodies, fixed in 4% PFA for 20 min at RT, rinsed with PBS, and then treated with 0.25% Triton X-100 at 4°C for 30 min, rinsed with PBS, and mounted for microscopy. In the STF protocol, detergent treatment preceded fixation.

Copatching Experiments

Antibody-induced cross-linking of various CKRs was carried out essentially as described (Harder *et al.*, 1998). Both primary antibody incubations were at 20°C for 5–10 min and secondary antibody reactions at 37°C for 5–10 min. CCR5 and KRFX were stained with unlabeled rabbit antiserum against CCR5 and CD71 mAb against Tfn-R, followed by fluorescent-labeled 2° antibody against rabbit and mouse IgGs, respectively. For X4 and X4-R5, cells were stained with unlabeled 1° antibody followed by fluorescent 2° antibody. Cells were then fixed and counterstained with fluorescent CD71 mAb for Tfn-R using rabbit antibodies for CCR5 and biotin-conjugated mAbs for CXCR4, followed by neutravidin-induced clustering.

Confocal Immunofluorescence Microscopy

Images were collected on a Leica TCS-NT/SP confocal microscope (Leica Microsystems, Exton, PA) using a 63 \times or 100 \times oil immersion objective NA 1.32, and digital zoom up to 2.2 \times . Fluorochromes were excited using an argon laser at 488 nm for Alexa 488 or FITC, a krypton laser at 568 nm for Alexa 568 or Texas Red (TR), and He/Ne laser at 633 nm for APC. Fluorescent emission from Alexa 350 dye and fillipin was visualized by excitation with UV laser. Detector slits were configured to minimize any cross-talk between the channels, or the channels were collected separately and later superimposed. DIC (differential interference contrast) images were collected simultaneously with the fluorescence images using the transmitted light detector. Twelve or more fields were examined per coverslip, and each experimental condition was repeated as indicated in the respective figure legends. Because not every field had equal representation of various expression patterns, the images shown in the figures were assembled from multiple fields. Fields showing colocalization were authenticated by confirming that at least five

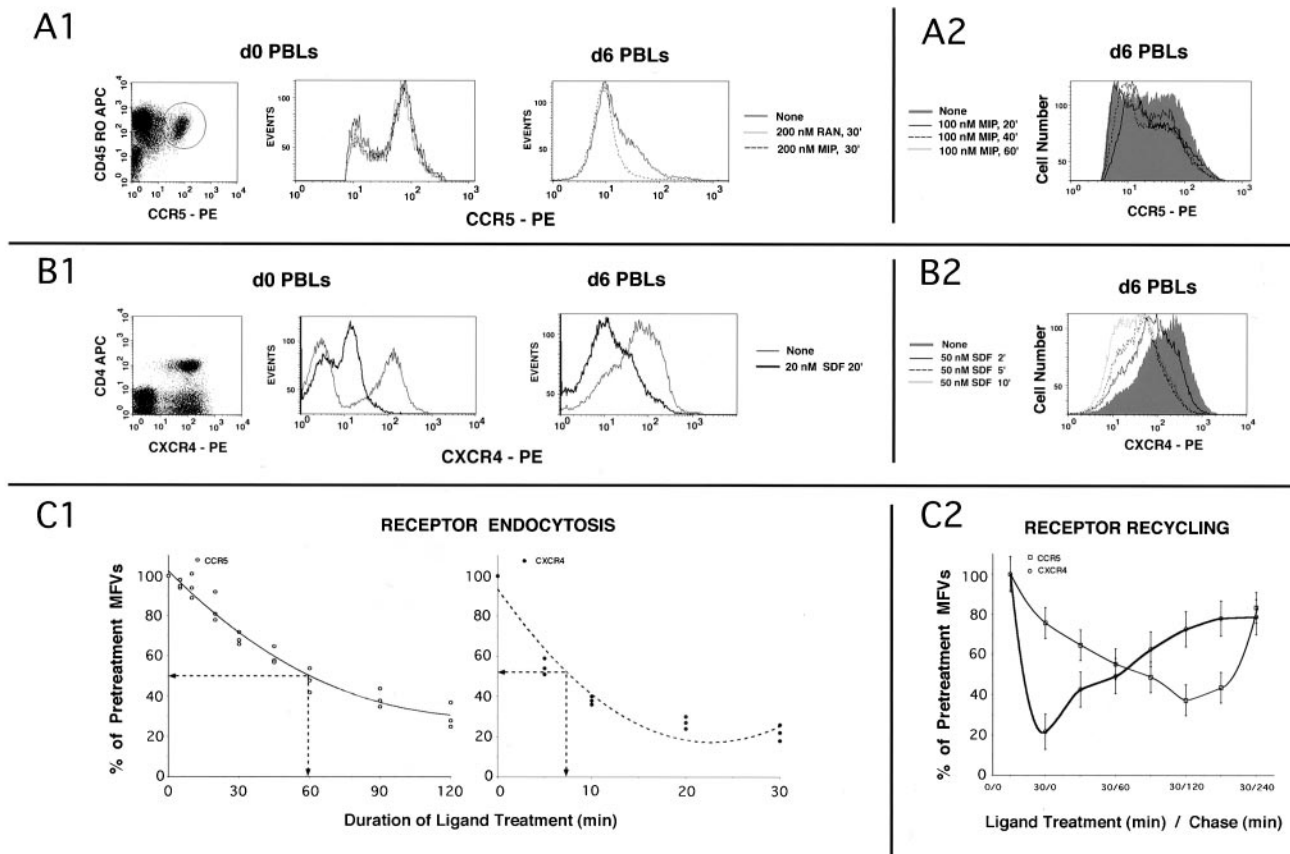


Figure 1. (A and B) Kinetics of agonist-induced internalization of CCR5 and CXCR4, respectively, in PBLs; (C) CKR internalization and recycling in expression systems. (A1) d0 PBLs represent CD4⁺ T cells. Bivariate analysis of the CD4⁺ subset stained with CCR5 mAb 3A9-PE and CD45RO-APC is shown on the left. CCR5⁺ subset is encircled. Cells were stimulated with RANTES (RAN), MIP-1 β (MIP) or untreated and the overlaid FACS histograms of the CCR5⁺ subset are shown immediately to the right. d6 PBLs are CD3 positive. Overlaid CCR5 histogram profiles of stimulated and untreated d6 PBLs are on the far right. (A2) Kinetics of MIP-1 β induced CCR5 downmodulation. Overlaid FACS histograms of cells treated for various times or untreated (shaded graph) are shown. CCR5 gating parameters were adjusted to exclude low-expressers (cutoff value of ~ 0.5 log). (B1) Bivariate analysis of CD3⁺ subset stained with CXCR4 mAb 12G5-PE; CD4-APC is on the left. CXCR4 histograms of d0 and d6 PBLs treated with SDF-1 α or untreated are shown in the next two panels. (B2) Kinetics of CXCR4 downmodulation by SDF-1 α . CXCR4 staining profiles of cells treated for various times or untreated (shaded graph) are shown. (C1) Receptor internalization using a HEK293 cell line expressing CCR5 and a cloned HeLa-CD4 line expressing high levels of CXCR4. Cells were stimulated with the respective chemokines (AOP-RANTES at 200 nM for CCR5; 20 nM SDF-1 α for CXCR4) for the indicated times, and the MFVs of different receptors were determined by FACS analysis. Data are expressed as percentage of initial MFVs as a function of duration of chemokine treatment. Data from three experiments were used to fit a polynomial curve. (C2) For receptor recycling experiments, cell lines (noted above) expressing the indicated receptor(s) were treated with protein synthesis inhibitors before and during the experiment. CCR5 was stimulated for 30 min at 100 nM of MIP-1 β and CXCR4 with 50 nM SDF-1 α . MFVs of receptors at various times during the experiment are plotted as percent of MFVs of pretreated cells on the ordinate (with error bars) with time of the experiment on the abscissa.

successive 0.15- μ m confocal planes displayed similar intensities of costaining. Running a colocalization algorithm module in the Leica software further validated such colocalized regions of interest. Images were processed using the Leica TCS-NT/SP software (version 1.6.585), Imaris 3.2.2 (Bitplane AG, Zurich, Switzerland), and Adobe Photoshop 7 (San Jose, CA).

RESULTS

CCR5 Undergoes Slower Endocytosis than CXCR4 upon Agonist Stimulation

We inquired whether the trafficking kinetics of CCR5 was distinct from that of CXCR4 in primary T cells. As shown in

Figure 1A1, CCR5-positive cells constituted 2–3% of T cells and were mostly in the long-term memory subset. CCR5 stimulation with two different CCR5 agonists (RANTES and MIP-1 β) at 200 nM for 30 min did not significantly alter the size or the MFV for this subset. During in vitro activation of T cells, there was a marked expansion in the CCR5⁺ subset reaching 20–25% by days 5–6. Agonist treatment induced reduction of high expressers, rather than quantitative loss of CCR5 on all these cells (Figure 1A1). In agreement with earlier reports (Mack *et al.*, 1998), the IC₅₀ and $t_{1/2}$ for AOP-RANTES was at least threefold better than for RANTES or MIP-1 β .

In contrast to CCR5, cell surface levels of CXCR4 on both d0 and d6 PBLs were downregulated 10-fold or more by stimulation with SDF-1 α at 20 nM for 20 min (Figure 1B1). We compared the kinetics of agonist driven internalization of both receptors on d6 PBLs. Cell surface CXCR4 density was progressively diminished by SDF-1 α treatment starting with 3-fold reduction within 2 min of stimulation and maximizing to >10 fold by 10 min (Figure 1B2). CCR5 was downregulated modestly on stimulation with 100 nM MIP-1 β for 20 min (Figure 1A2), with a greater loss of high expressers rather than a substantial reduction in the MFV. The sluggish internalization of agonist-treated CCR5 did not result from reduced binding affinity. Tenfold lower concentrations of either CCR5 agonist (10 nM AOP-RANTES or 20 nM MIP-1 β) elicited maximal signaling response (by intracellular Ca²⁺ flux) from CCR5 instantaneously and rapidly induced desensitization (<1 min). The above findings were reproduced with PBLs from eight different donors. From these data, we concluded that the agonist IC₅₀ for internalization of CCR5 was at least 10-fold higher than for CXCR4 in primary T cells.

To study the mechanism governing the difference in CCR5 and CXCR4 internalization, we used an HEK293 cell line stably expressing CCR5 and a cloned HeLa CD4 cell line with high CXCR4 expression. Individual cells were treated with IC₂₅ concentrations of the respective ligands, and cell surface receptor MFVs were monitored periodically by FACS. At 20 nM SDF-1 α , CXCR4 density was reduced fivefold, with a $t_{1/2}$ of 7 min (Figure 1C1, right panel). In contrast, CCR5 (left panel) underwent sluggish internalization on treatment with 200 nM AOP-RANTES, asymptotically approaching 30–40% of initial values with a $t_{1/2}$ of 60 min. As for PBLs, the agonist concentrations required for discernable internalization were 5–10-fold higher than the levels that elicited maximal signaling and desensitization (unpublished data). Similar differences in the $t_{1/2}$ values for CCR5 and CXCR4 were observed with HOS cells stably expressing these receptors (unpublished data). Thus the receptors behaved similarly in these model systems and in primary T cells.

Rates of recycling of agonist-treated CCR5 and CXCR4 were determined in stable cell lines that had been treated to block de novo protein synthesis. As before, CXCR4 underwent substantial downregulation after 30 min of SDF-1 α treatment (Figure 1C2). It began to recycle to the cell surface immediately after agonist removal, and within 3 h reached 80% of pretreatment levels. In contrast, internalization of CCR5 was sluggish during the initial 30 min of MIP-1 β treatment and continued slowly during the first 2 h after removal of the agonist. During the next 2 h, CCR5 began to recycle slowly back to the cell surface, reaching 80% of pretreatment levels. The above experiments were repeated using HOS cell lines expressing CCR5 or CXCR4 with similar results (unpublished data). Thus, although the kinetics of internalization was different for CCR5 and CXCR4, both of them recycled to the plasma membrane.

To further evaluate the extent of internalization, we used confocal microscopy to monitor the agonist-driven internalization of fluorescent mAbs bound to the cell surface receptors. In HOS cells stably expressing CCR5, almost all of the receptor remained at the cell surface after agonist treatment (Figure 2A). A small fraction of CCR5 antibodies was inter-

nalized in both treated and untreated cells, and colocalized with Tfn-loaded vesicles, probably representing intrinsic recycling of the receptor. However, upon prolonged agonist treatment (200 nM MIP-1 β for 90 min), CCR5 was internalized and partially colocalized with Tfn-loaded endosomes (Figure 2A, right). In contrast, both SDF-1 α and PdBu treatments induced substantial internalization of surface-bound CXCR4 mAb, which colocalized with Tfn-loaded vesicles (Figure 2A) within 20 min. PdBu treatment resulted in a more complete transfer of CXCR4 to the endosomes, consistent with previous reports (Signoret *et al.*, 1998; Orsini *et al.*, 1999) showing that CXCR4 but not CCR5 was susceptible to phosphorylation and internalization by PKC activation induced by PMA (or PdBu). PdBu (or PMA)-treated CXCR4 undergoes phosphorylation at sites different from those induced by SDF binding. It is likely that CXCR4 internalized by PMA treatment does not get dephosphorylated or recycled, exaggerating the accumulation of PdBu-treated CXCR4 in the endosomal compartment.

The sluggish CCR5 trafficking was also observed in an HEK293 cell line stably expressing CCR5 and in a HeLa cell transient expression system. CXCR4 on the other hand exhibited rapid transport in many epithelial cells. Because we found no obvious defect in CXCR4 endocytosis in these cells, we inquired whether the trafficking phenotype of other CKRs was more like CCR5 or CXCR4. CCR3 in a HOS cell line and CXCR1 in HeLa transfectants were mobilized readily from the cell surface and the internalized receptors colocalized with Tfn-bearing vesicles on stimulation with their respective ligands (Figure 2B). This led us to conclude that the slow retrograde trafficking of CCR5 was a property specific to this receptor rather than a general property of the cell system in which it is expressed.

Role of C-tail of CCR5 in Regulating Endocytosis

We have shown before that sequential truncations of the cytoplasmic tail of CCR5 caused a progressive decrease in CCR5 trafficking to the cell surface, and the anterograde trafficking was severely perturbed by a truncation that excised the palmitoylated cysteine residues (Venkatesan *et al.*, 2001). We inquired whether C-terminal domain(s) modulate retrograde trafficking of agonist-occupied CCR5 in a similar manner. Cell surface density of wt CCR5 and of CCR5 truncated to the 324th residue (tCCR5) was unaffected by agonist treatment. However, agonist treatment downmodulated (about threefold) the cell surface expression of the KRFX mutant that lacks the palmitoylation motif (Figure 3B). These CCR5 mutants were competent for chemokine binding and activation of G α i-mediated signaling pathway leading to intracellular calcium flux (Venkatesan *et al.*, 2001). However, the duration of the functional response and the late events were severely affected for the nonpalmitoylated mutant (Blanpain *et al.*, 2001).

The FACS results were corroborated by confocal microscopy. wt CCR5 and two successive C-terminal truncations to the 348th or the 335th residue were internalized poorly (if at all) by MIP-1 β treatment. CCR5 truncated to the 324th residue underwent partial mobilization from the cell surface (Figure 4A) with some evidence of colocalization of this internalized mutant with Tfn in the endosomes. In contrast, the KRFX mutant exhibited brisk mobilization from the cell surface after agonist treatment colocalizing with Tfn-loaded

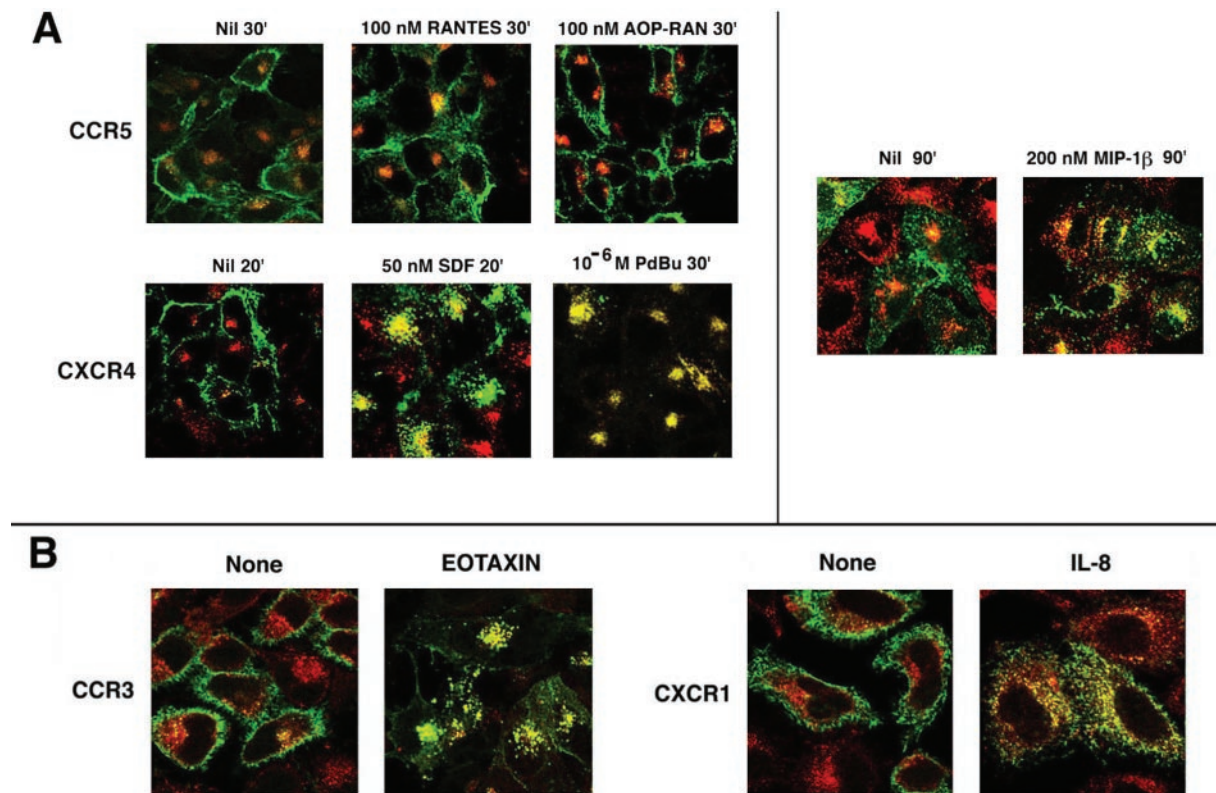


Figure 2. Agonist-mediated CCR visualized by confocal microscopy. In all cases, Tfn-R endocytosis was monitored by Tfn-TR, shown in red. (A) Ligand mediated endocytosis of CCR5 and CXCR4 using HOS cell lines (images on the left) or HeLa cell transfectants (images on the right). CCR5 and CXCR4 were visualized by APC-labeled 3A9 and 12G5 mAb, respectively. The various ligand treatments and durations are denoted at the top of each image. Results represent three or four experiments. (B) Trafficking pattern of CCR3 and CXCR1 after exposure to their cognate ligands appropriately identified. Endocytosis assay was with HeLa cell transfectants. CCR3 and CXCR1 trafficking was visualized by use of FITC-conjugated mAbs. The respective agonists were used at 100 nM for 30 min. Results represent two experiments.

endosomes (Figure 4A, compare the cell surface vs. endosomal distribution of agonist-occupied KRFX with those of more distal truncations or the wt receptor on the right).

In contrast, excision of the C-tail of CXCR4 (tCXCR4) did not significantly alter cell surface expression of the receptor (Figure 3B), and tCXCR4 was poorly internalized by SDF-1 α (Figure 4B) as shown elsewhere (Haribabu *et al.*, 1997). The central cluster of yellow vesicles (tCXCR4 colocalized with Tfn) probably represents intrinsic receptor recycling because a similar pattern was also observed in untreated cells expressing various receptors (for example, see untreated X4-R5 in Figure 4B). Cell surface expression and signaling of an X4-R5 chimera exchanging the C-tail of CXCR4 for that of CCR5 was similar to that of wt CXCR4 (Venkatesan *et al.*, 2001). The cell surface density of X4-R5 after SDF-1 α treatment was not reduced as demonstrated by the FACS histogram in Figure 3B. The poor trafficking of SDF-1 α occupied X4-R5 was obvious in the confocal microscopy assay under conditions that caused almost quantitative endocytosis of wt CXCR4 (Figure 4B). X4-R5 underwent endocytosis only after prolonged SDF treatment at 200 nM, much like the wt CCR5 with its cognate ligand (Figure 2A). Similar studies with a reciprocal CCR5 chimera (R5-X4), exchanging the C-tail of CCR5 for that of CXCR4, were not possible since such an exchange markedly diminished cell surface expression of

the chimera (Venkatesan *et al.*, 2001). The above findings led us to conclude that the trafficking of the agonist-bound KRFX mutant lacking the palmitoylation motif was considerably improved over that of wt CCR5 or that of distal CCR5 truncations that preserved the palmitoylation motif. Conversely, an intact C-tail of CCR5 transferred the sluggish trafficking phenotype of CCR5 to the X4-R5 chimera.

CCR5 Internalization Is Rab5 Dependent

Efficient trafficking of receptors to early endosomes requires the function of rab5 GTPase and a GDP bound dominant negative rab5 (S34N, -) mutant inhibits this process (Stenmark *et al.*, 1994). We investigated the effect of overexpressing wt or mutant forms of rab5 on the trafficking of various CKRs and Tfn receptor. In HeLa cells overexpressing wt rab5, there was a modest increase in the internalization of agonist-occupied CCR5 (Figure 5). This was more pronounced in cells expressing the hyperactive rab5 (Q79L mutant, ++), where most of the CCR5 colocalized with Tfn in morphologically distinct vesicles (Stenmark *et al.*, 1994, 1996). It is not clear whether this reflects enhanced agonist-mediated endocytosis, because there was significant internalization of CCR5 in rab5 (++) cells even in the absence of agonist (our unpublished results). In cells expressing the

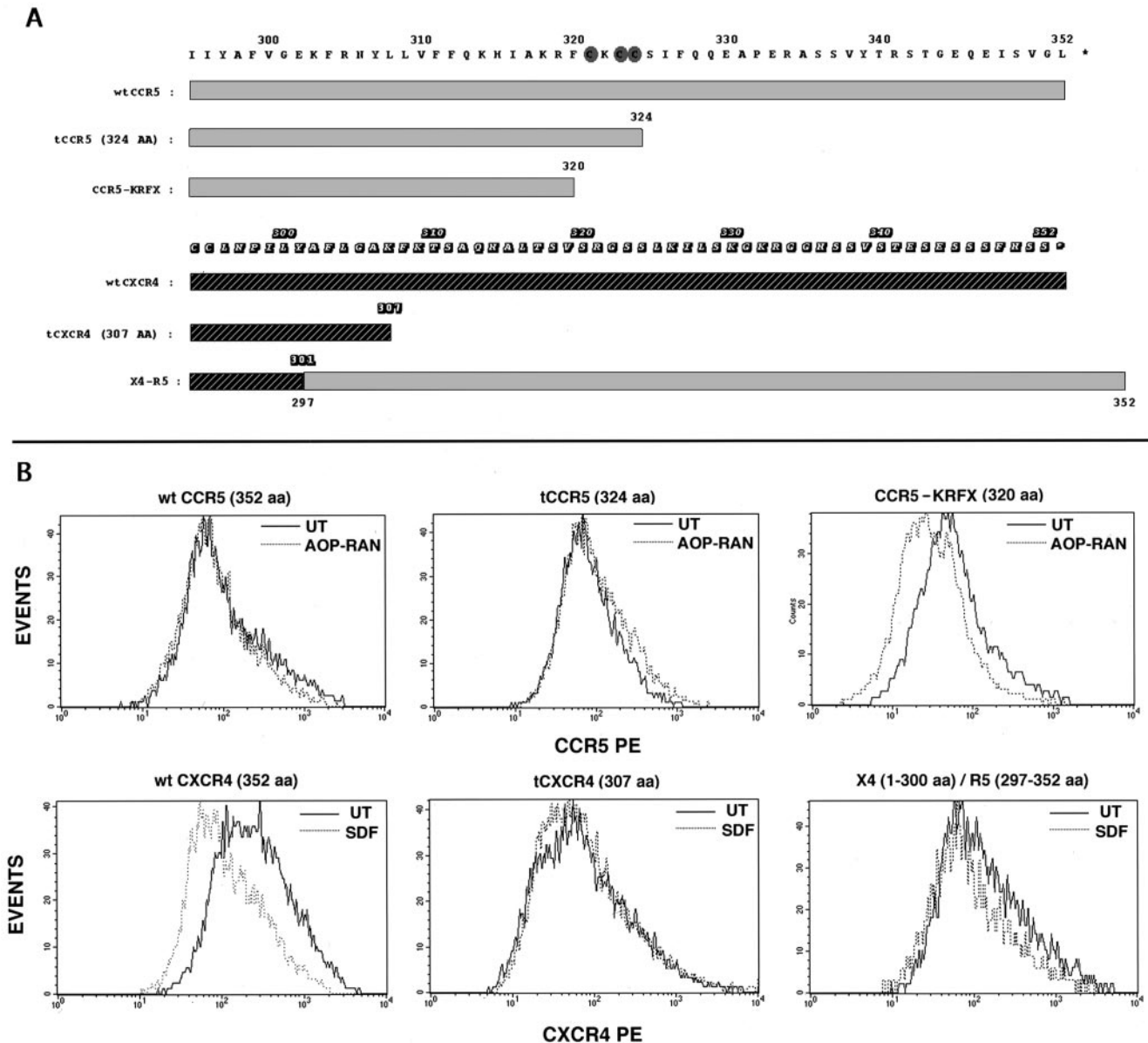


Figure 3. (A) Sequence alignment of the C-tails of CCR5, CXCR4, and derivatives. C-terminal domains of CCR5 and CXCR4 and deletions are denoted by the different shaded rectangles with the numbered amino acid sequence above. The CCR5 and CXCR4 coordinates of X4-R5 are denoted by dual shaded rectangles. Shaded ovals highlight the cysteines in the palmitoylation motif of CCR5. (B) Effect of agonist treatment on the cell surface density of CKRs. HEK293-T cells cotransfected with CD8 and the respective CKRs were treated with the appropriate agonists or untreated and stained for CD8 and CKRs. Histogram profiles of CKR densities in CD8-gated populations are shown. CCR5, tCCR5, and KRFX were stained with a mixture of CD8-APC and 3A9-PE. Agonist (AOP-RAN) treatment was at 200 nM for 30 min. CXCR4 and its derivatives were stained with CD8-APC and 12G5-PE. SDF-1 α treatment was at 100 nM for 20 min. Results represent three experiments.

dominant negative (GDP bound) form of rab5 (S34N mutant, -), CCR5 remains predominantly cell surface bound after agonist treatment (Figure 5). wt or hyperactive rab5 did not materially accentuate an already efficient endocytosis of CXCR4 after SDF-1 α treatment. On the other hand, there was a significant diminution of endocytosis of Tfn-R and CXCR4 in cells expressing dominant negative rab5. The trafficking phenotype of the X4-R5 chimera was essentially like that of CCR5 in the various rab5-expressing

cells. Thus both CCR5 and CXCR4 appear to be destined to endosomes after agonist stimulation.

Internalization of CXCR4 and CCR5-KRFX Occurs by a Clathrin-dependent Process

We next investigated the pathways that these receptors take to early endosomes. Because recruitment of the receptors

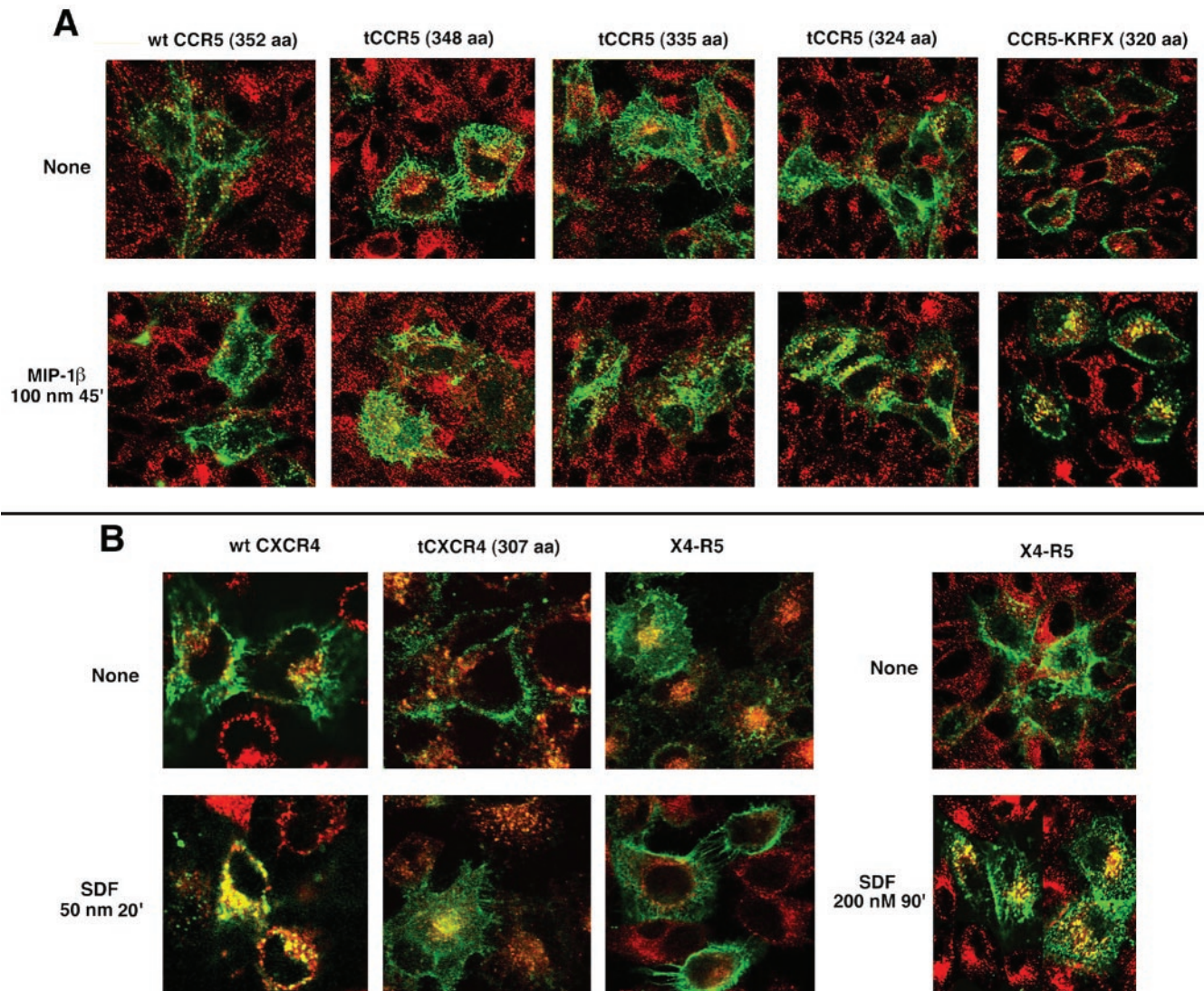


Figure 4. Endocytic patterns of agonist-stimulated CCR5, CXCR4, and their derivatives. Tfn-TR monitored Tfn-R trafficking. The receptors are colored green and Tfn-R in red. Images representing three experiments are shown. (A) Endocytosis pattern of AOP-RANTES (100 nM, 30 min) treated or untreated transfectants expressing wt CCR5 and serial C-terminal truncations. 3A9-APC staining visualized CCR5. (B) Endocytosis pattern of SDF-1 α (50 nM, 30 min) treated or untreated cells expressing wt CXCR4, tCXCR4, or X4-R5. CXCR4 was visualized by staining with 12G5-APC. Trafficking pattern of X4-R5 chimera treated with 200 nM SDF for 90 min is shown by the images on the extreme right.

into clathrin-coated vesicles is classically the earliest step in endosomal traffic, perturbation of Rab5 function that affects distal steps in endosome fusion would not be rate limiting for this process. Furthermore, receptors trafficking via clathrin-independent routes eventually fuse with early endosomes. Therefore, we targeted Eps15 protein, a key proximal regulator of CCV assembly. As expected, a substantial fraction of wt CCR5 remained on the cell surface after MIP-1 β treatment in Eps15 nonexpressers (Figure 6A, double closed arrowheads), although some cells displayed somewhat better endocytosis (double open arrowheads), which suggested that a small fraction of CCR5 was endocytosed in a clathrin-dependent manner. Tfn uptake was inhibited in inverse

correlation with Eps15 mutant expression levels (Figure 6A, arrows, Tfn panels). Agonist driven internalization of CXCR4 exhibited a similar pattern in Eps15 mutant expressing cells (Figure 6A, arrows). Likewise, trafficking of another CXC receptor, CXCR1 that is normally rapidly internalized upon ligand (IL-8) treatment was inhibited by Eps15 mutant coexpression (Figure 6A, arrows). More significantly, the Eps15 mutant also reduced the magnitude of endocytosis of agonist-treated CCR5-KRFX (Figure 6A, arrows). In the Eps15 mutant cells, there appeared to be an inverse correlation between Eps15 mutant expression and the total expression levels of some CKRs and Tfn. However, this was not the case for CCR5 transfectants, which displayed roughly equiv-

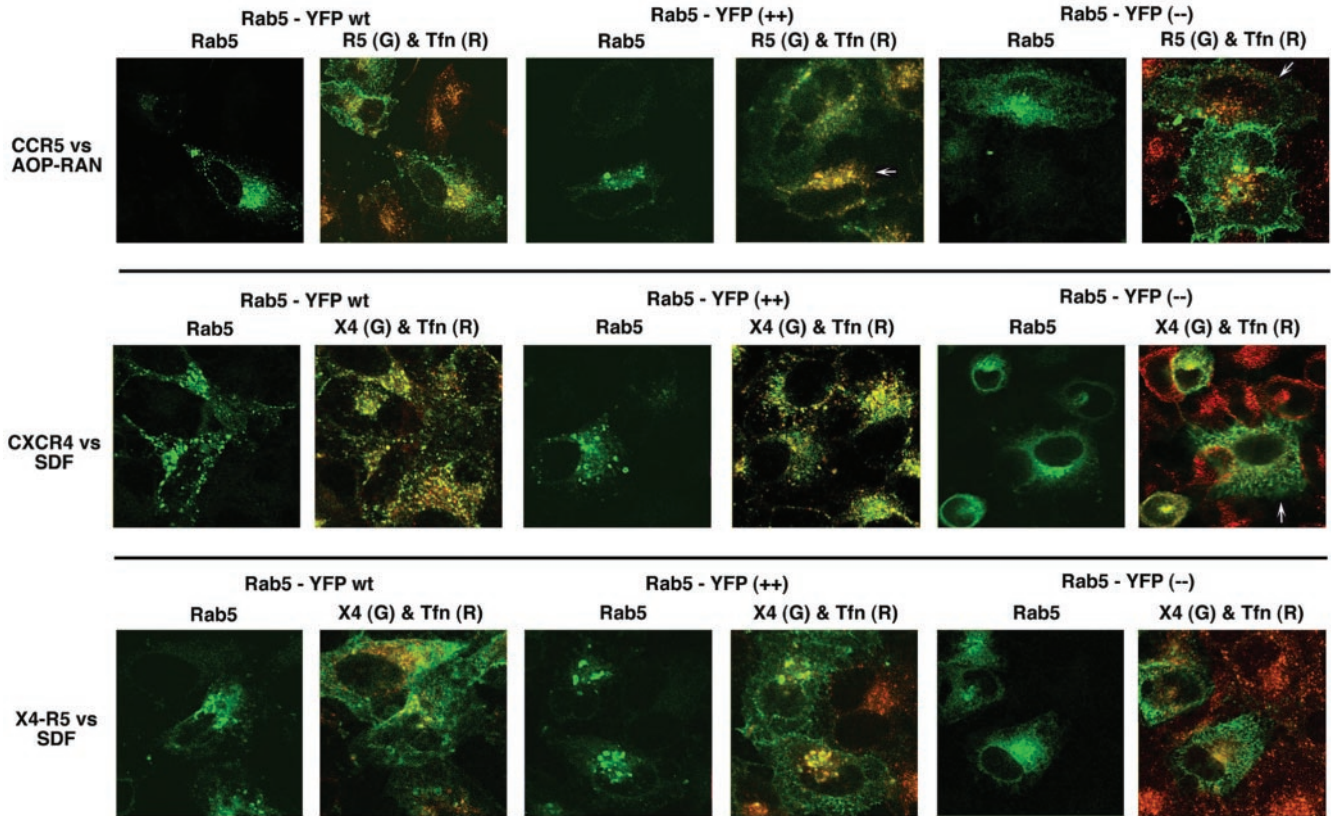


Figure 5. Agonist-driven endocytosis of CKRs in the context of wt and mutant rab5 expression. HeLa cells were cotransfected with the indicated CKRs (CKR) and wt, Q79L (++), or S34N (–) versions of rab5-YFP proteins. Tfn-TR was used to monitor Tfn-R traffic. Each row shows results obtained with a particular receptor/ligand combination. In each case, RGB images were processed to display side-by-side rab5-YFP image in green and the overlaid image of CKR in green and Tfn in red. CCR5 was stimulated with AOP-RANTES (100 nM for 30 min); CXCR4 or X4-R5 with SDF-1 α . 3A9-APC and CXCR4 and X4-R5 visualized CCR5 by 12G5-APC. Images represent three experiments.

alent levels of Eps15 mutant and CCR5 (mostly at the cell surface), reflecting the sparse endocytosis of CCR5 with limited agonist treatment. With the CKRs and Tfn-R that undergo brisk clathrin-dependent endocytosis, stalled trafficking in the Eps15 mutant cells possibly redistributes most of the agonist-treated receptors diffusely under the plasma membrane, rather than in vesicles, thus rendering their imaging difficult. FACS analysis and confocal imaging indicated that there was no appreciable difference in the average cell surface density of various receptors between untreated cells expressing EGFP vs. EA95–295 (unpublished data). Thus, the above results confirmed that endocytosis of CXCR1, CXCR4, and the KRFX CCR5 mutant followed a clathrin-dependent pathway like the well-characterized Tfn-R trafficking.

Agonist-occupied CXCR4 and the KRFX CCR5 Mutant, But Not wt CCR5 are Internalized Rapidly and Colocalize with Clathrin Vesicles

We compared the cell surface and intracellular distribution of wt and KRFX-CCR5 and CXCR4 with that of clathrin at various times after agonist treatment. Cells were labeled

with the appropriate receptor-specific antibodies and exposed to their cognate agonists. At various times, cells were fixed and permeabilized and stained to visualize clathrin vesicles and internalized receptor antibodies. Internalization of CXCR4 began within 2 min and was essentially completed by 10–20 min. During this time frame, there was significant colocalization of CXCR4 with clathrin, reflecting a rapid transit to the endosomes (Figure 6B). Trafficking of agonist-bound KRFX mutant of CCR5 followed an essentially similar pattern, albeit at slower pace. In contrast, agonist-bound wt CCR5 was not mobilized from the plasma membrane in this time frame, and only at ~40 min after agonist treatment was there some evidence of CCR5 internalization (Figure 6B).

Because the lack of colocalization of agonist-occupied CCR5 with clathrin does not formally exclude delayed trafficking via clathrin cages, we inquired whether CCR5 endocytosis induced by protracted agonist treatment at 200 nM (Figure 2A) followed a clathrin-dependent pathway. We compared internalization of agonist-occupied CCR5 with that of Tfn-R in cells coexpressing dominant inhibitors of the clathrin pathway, namely the EA95/295 Eps15 mutant de-

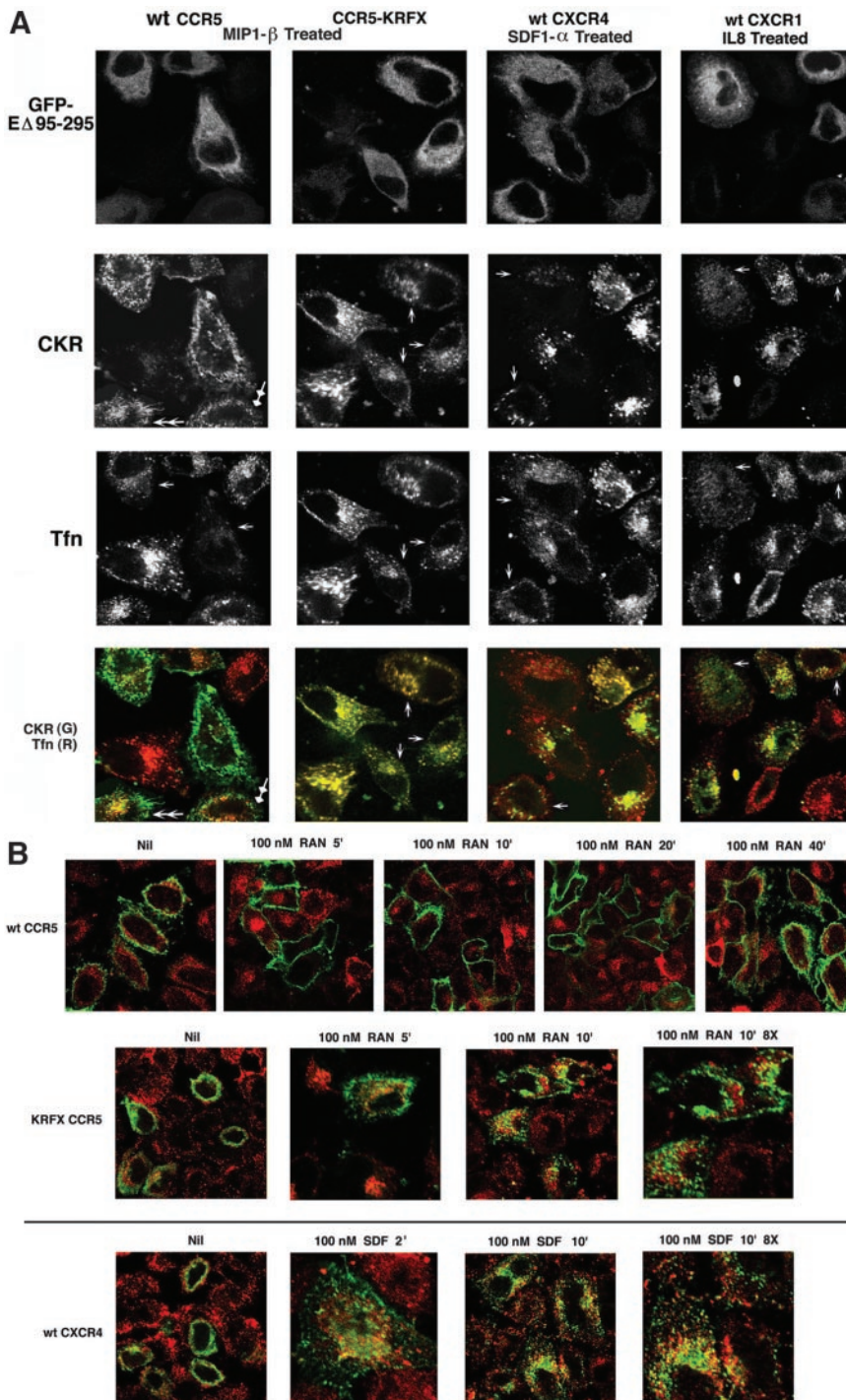
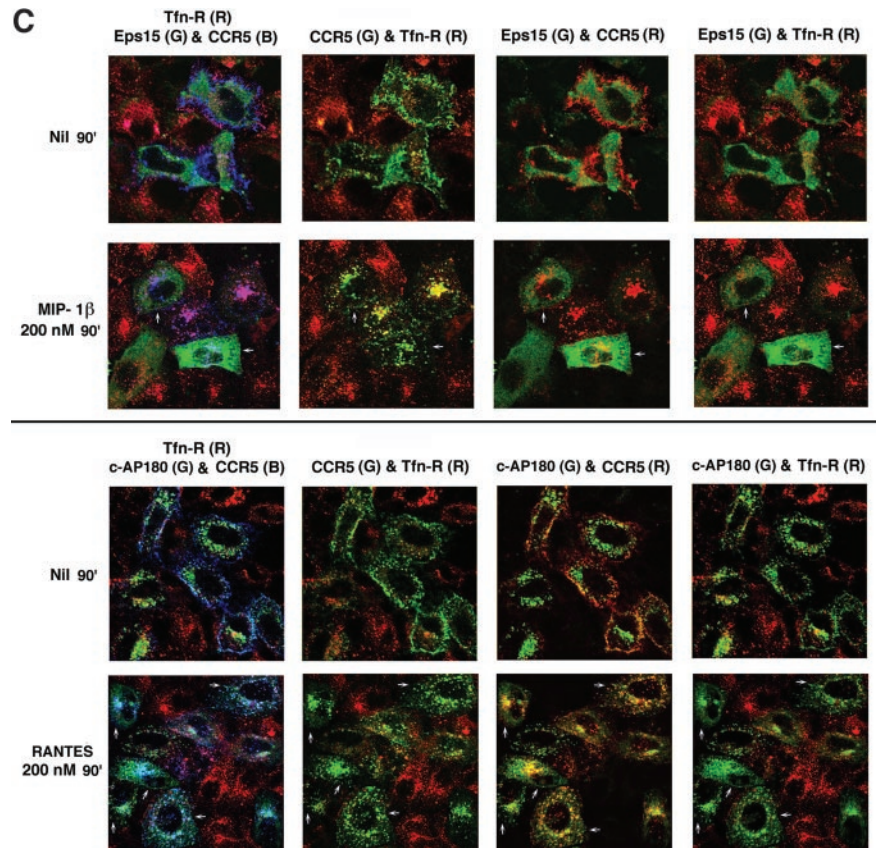


Figure 6.

scribed above or the C-terminal fragment of the clathrin adapter, AP180 (Ford *et al.*, 2001), tagged with a FLAG epitope. Confocal images representing three experiments are shown in Figure 6C. In cells expressing either inhibitor, Tfn uptake was markedly reduced or virtually absent (Figure 6C, right column, top and bottom panels) whether or not the cells were treated with the indicated CCR5 agonist. Al-

though in cells expressing the Eps15 mutant, there was a dose-dependent reduction of Tfn uptake (Figure 6C, top panel, 2nd and 4th columns); Tfn uptake was more efficiently blocked in the c-AP180 cells (Figure 6 C, bottom panel, 2nd and 4th columns). In contrast, there was significant residual endocytosis of CCR5 after 90-min treatment with 200 nM MIP-1 β in E Δ 95/295 expressers (Figure 6C, top

Figure 6 (continued from facing page). (A) Effect of dominant negative Eps15 on agonist-driven endocytosis of wt CCR5 and KRFX mutant; wt CXCR4 and CXCR1. HeLa cells were cotransfected with GFP-tagged Eps15 mutant, E Δ 95/295, and the indicated chemokine receptors (CKR). Chemokine receptor trafficking was initiated by agonist treatment (MIP-1 β for wt and CCR5-KRFX, SDF-1 α for wt CXCR4, and IL8 for CXCR1) at 100 nM for 30 min. APC-conjugated 3A9 or 12G5 mAb was used to visualize trafficking of CCR5 and KRFX or CXCR4, respectively. CXCR1 was stained with unconjugated mAb followed by 2 $^{\circ}$ staining of fixed and permeabilized cells with APC-conjugated anti-mouse IgG. TR-conjugated Tfn was used to monitor Tfn-R trafficking. Each column represents results obtained with the individual receptor/agonist combinations that are denoted at the top. RGB images were separated into individual channels corresponding to GFP-E Δ 95/295, CKR, and Tfn and laid out in successive rows. The bottom panels show overlaid images corresponding to CKR (green) and Tfn (red). Arrows denote cells described in text. Photomultiplier gains were adjusted to visualize faint vesicles labeled with Tfn or CKR. (B) Time course of colocalization of agonist-occupied chemokine receptors with clathrin vesicles. HeLa cells transfected with the indicated receptors were treated with their cognate agonists for the indicated times or left untreated. Endocytosis was evaluated by confocal microscopy. Cells were preincubated with rabbit IgG against the N-terminal peptides of CCR5 or CXCR4 at 4 $^{\circ}$ C for 15 min, before agonist treatment for the indicated times. Fixed and permeabilized (in 0.1% Triton X-100) cells were stained with mAb against human clathrin heavy chain. 2 $^{\circ}$ staining was with a mixture of Alexa 488- and 568-conjugated anti-rabbit and anti-mouse IgG. Nil denotes cells without agonist for the entire duration of the assay. Images were pseudocolored to show the receptors in green and clathrin in red. All images in this figure were at 2 \times digital zoom using a 63 \times objective, except for those denoted as 8 \times . (C) Endocytic trafficking patterns of ligand bound CCR5 and Tfn-R in the context of interference of clathrin pathway by the dominant negative E Δ 95/295 mutant (Eps15) or the C-terminal fragment of AP180 (c-AP180). HeLa cells were cotransfected with CCR5 and GFP-tagged E Δ 95/295 mutant (top panel) or FLAG-tagged c-AP180 (bottom panel). TR-conjugated Tfn illuminated Tfn-R trafficking. The top and bottom rows of each panel show results obtained without or with CCR5 chemokine treatments, respectively. The left column is a composite of images showing CCR5 mAb conjugated with APC (CCR5; B), Tfn-R in red, and GFP-tagged, E Δ 95/295 (Eps15; G) in the top panel or c-AP180 stained with rabbit anti-FLAG IgG followed by Alexa 568 conjugated 2 $^{\circ}$ antibody in the bottom panel. Pseudocolored images representing CCR5 in green and Tfn-R in red; CCR5 in red and Eps15 mutant or c-AP180 in green; and Tfn-R in red and Eps15 mutant or c-AP180 in green are shown in the successive columns on the right. Arrows denote cells described in text.



panel) or with RANTES treatment in c-AP180 expressers (Figure 6C, bottom panel). For instance, in cells expressing either inhibitor and that have been treated with agonist (some expressers are denoted by arrows), CCR5-containing vesicles appear predominantly green, because no Tfn was internalized in these cells. By contrast, in cells that do not express the clathrin inhibitor(s), CCR5-bearing vesicle are yellow or orange, reflecting colocalized Tfn. From these experiments we concluded that a substantial fraction of agonist-occupied CCR5 followed a clathrin-independent itinerary.

The C-tail of CCR5 Determines Receptor Localization to Plasma Membrane Rafts

Receptors with acylated C-tails tend to accumulate in lipid rafts (Melkonian *et al.*, 1999). The slow retrograde

traffic of agonist-driven CCR5 and X4-R5 might reflect the preferential distribution of these receptors in such domains. We tested this hypothesis using three complementary methods. First, we depleted cholesterol from lipid rafts by treating cells with CyDx (Keller and Simons, 1998) or fillipin (Orlandi and Fishman, 1998). Treatment with increasing concentrations of CyDx led to a progressive loss of cholesterol from HeLa cells (Figure 7A) and other cell types. As an alternative, we also extracted cholesterol from the cells by treatment with fillipin (10 μ g/ml). Both CyDx and fillipin extraction of cholesterol resulted in a threefold loss in cell surface CCR5 density in HeLa transfectants (Figure 7B) and HEK-293 and HOS cell lines stably expressing CCR5 (unpublished data). In contrast, cell surface levels of palmitoylation-deficient CCR5-KRFX or CXCR4 were unaffected by either treatment. CyDx induced a modest loss in the cell surface levels of the

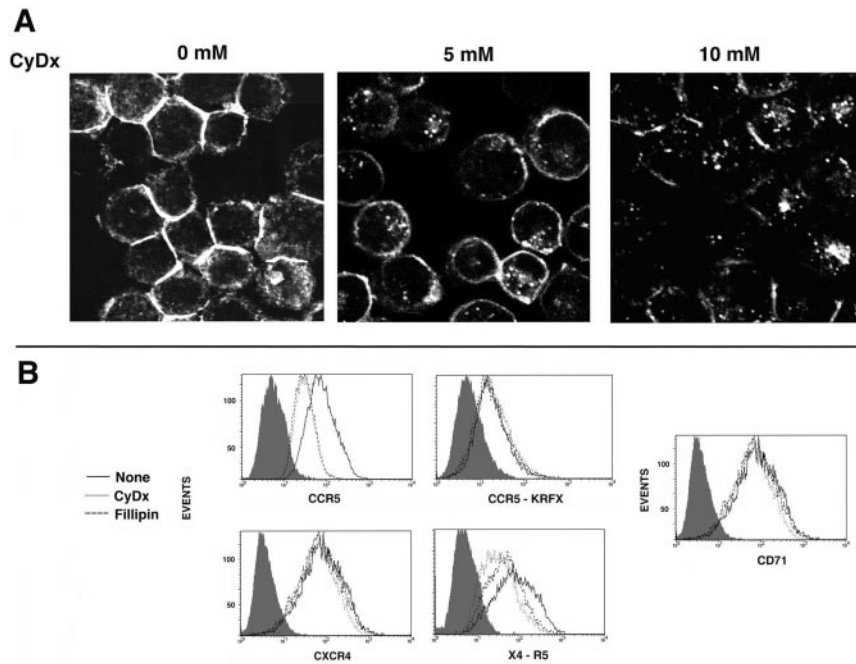


Figure 7. Cholesterol depletion by methyl- β -cyclodextrin (CyDx) and its effect on cell surface density of CKRs. (A) Cholesterol staining of CyDx-treated HeLa cells. After treatment, cells were fixed and stained for cholesterol with fillipin (10 μ g/ml) for 10 min at RT and visualized by UV laser microscopy. (B) FACS histograms of CKR expression in HeLa cell transfectants treated with CyDx (5 mM) or fillipin (10 μ g/ml) or left untreated. CD4 was cotransfected in each case to monitor expression. Transfectants were stained with CD4-APC and PE-conjugated mAbs for the respective receptors, except for the KRFX mutant. Because transport of this mutant to the cell surface was quite poor, cells were stained with unconjugated 1 $^{\circ}$ mAbs followed by PE-conjugated 2 $^{\circ}$ antibodies. Cells were gated for CD4 staining because it was not altered by cyclodextrin or fillipin treatment. Histogram profiles of CKR densities in CD4-gated populations representing two experiments are shown. Shaded histograms represent staining with an isotypic control.

X4-R5 chimera. Tfn-R (CD71), which does not localize to rafts, was resistant to cholesterol extraction. These results suggested that the palmitoylated C-tail of CCR5 anchored the receptor in the raft domains.

Second, we carried out copatching experiments using CTx-B, which binds to GM1 ganglioside in rafts, and antibodies against Tfn-R, a nonraft marker (Harder *et al.*, 1998). For examining colocalization of CKRs with Tfn, HeLa cell transfectants expressing the receptors were simultaneously incubated with FITC-labeled CCR5 or CXCR4 mAb and CD71-APC for Tfn-R followed by anti-mouse IgG. The patches of wt CCR5 and CXCR4 remained largely segregated from the clustered Tfn-R (Figure 8A). The KRFX mutant and the X4-R5 chimera displayed a similar pattern, with the latter occasionally copatching with Tfn-R.

GM1 ganglioside is a major component of raft microdomains and CTx-B, which is pentavalent for GM1, induces clustering of GM1 (Harder *et al.*, 1998). We carried out copatching experiments by staining the HeLa transfectants with unlabeled CCR5 or CXCR4 mAb and Alexa 594-conjugated CTx-B followed by labeled 2 $^{\circ}$ antibody staining. CCR5 but not CXCR4 or KRFX colocalized with CTx-B (Figure 8A). Furthermore, the X4-R5 chimera also copatched with the GM1 clusters, indicating that the palmitoyl motif of the C-tail of CCR5 is the dominant determinant of raft association.

Third, we used detergent extraction as a test of CCR5 association with the plasma membrane rafts. Proteins associated with detergent insoluble glycolipid-enriched membrane fractions (DIGs or DRMs) isolated by a batch method or flotation gradients are considered to be raft proteins (Simons and Ikonen, 1997, 2000; Brown and London, 1998). Nevertheless, biochemical fractionation of candidate receptors into DIG fractions does not always reflect their actual organization at the plasma membrane.

Acquisition of raft affinity may be variable for different GPCRs and partly determined by the slow rate of their biosynthetic transport, because receptors stalled in the ER/Golgi en route to the plasma membrane may not be raft associated (Scheiffele *et al.*, 1997). Furthermore, palmitoylation of receptors that reinforces raft association probably occurs at the plasma membrane (Berthiaume and Resh, 1995). Therefore, we examined by fluorescence microscopy the cell surface distribution of various receptors before and after detergent extraction using HeLa cell transfectants. Images of cells stained with fluorescent mAbs followed by fixation and detergent extraction (Stain, Fix, TXT) were compared with those of cells that were stained and extracted with Triton X-100 before fixation (Stain, TXT, Fix). Cell surface staining of CD4 or CCR5 in HeLa cells was not significantly altered whether the cells were extracted with detergent before or after fixation, thus qualifying them as raft proteins (Figure 8B). In contrast, there was a greater loss of cell surface CXCR4 staining in detergent extracted cells. As expected, Tfn-R was highly sensitive to detergent extraction.

Agonist-treated CCR5 Is Internalized into Caveolin-positive Vesicles by Largely Clathrin-independent Pathways

A number of signaling receptors and monomeric and trimeric G proteins have been isolated as large signaling complexes in lipid rafts (Simons and Toomre, 2000). Caveolae are one such domain implicated in diverse cellular trafficking and signaling mechanisms (Anderson, 1998). We inquired whether CCR5 caveolae were involved in CCR5 or CXCR4 endocytosis by both structural and functional tests using HeLa cells transfected with receptor expression plasmids. To reduce the cell surface background, transfectants were acid washed to strip noninternalized antibody. As

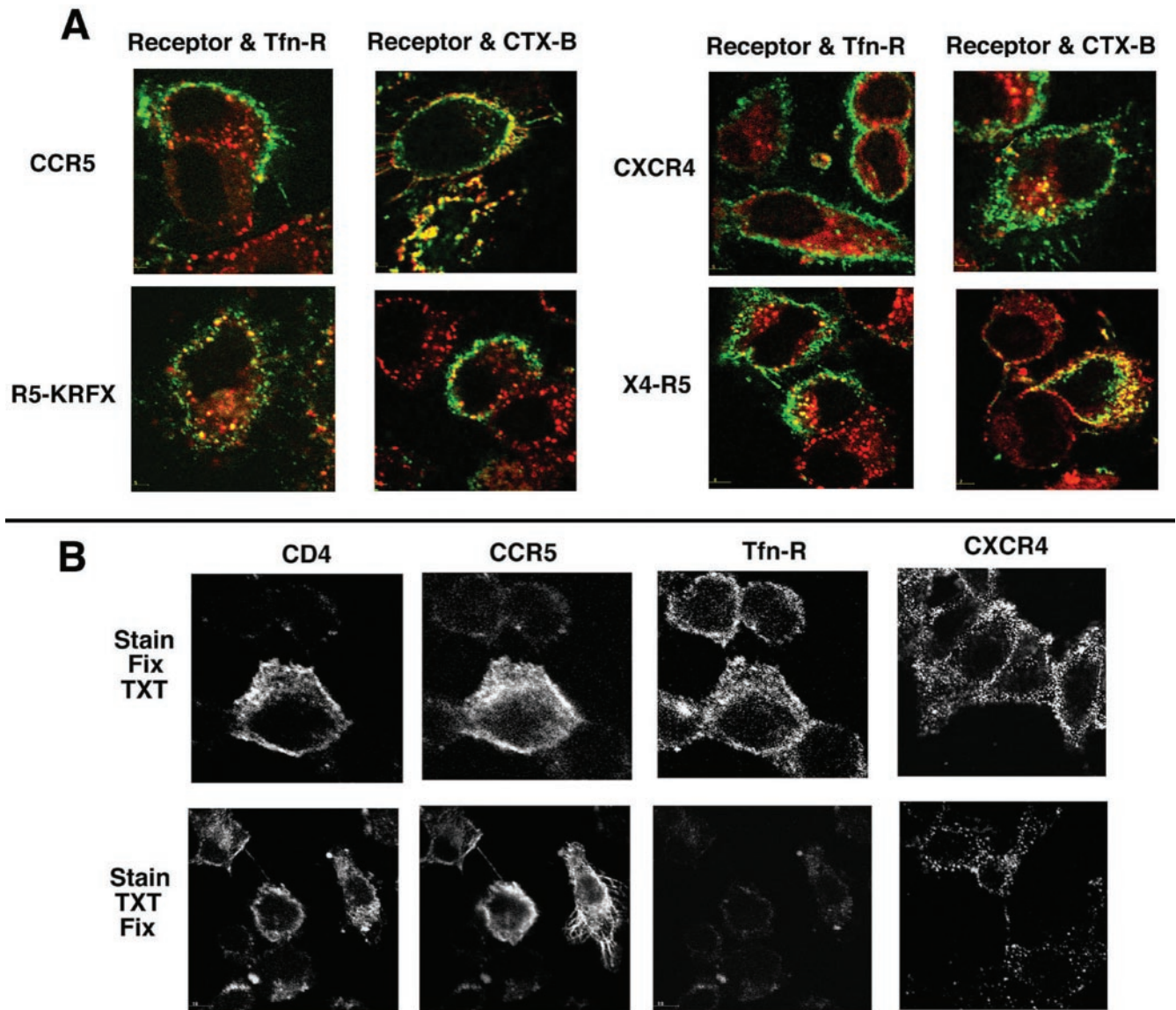


Figure 8. (A) Copatching of CCR5, CXCR4, and derivatives with raft and nonraft markers. HeLa cells transfected with wt CCR5, KRFX, CXCR4, or X4-R5 were stained at 20°C for 10 min with FITC-labeled 2D7 (for CCR5 and KRFX) or 12G5 mAbs for wt and KRFX-CCR5 or CXCR4, respectively; CD71-APC followed by cross-linking with anti-mouse IgG. For copatching with CTx-B, cells were costained with Alexa 594-CTx-B and unlabeled 2D7 or 12G5 mAb at 20°C for 15 min followed by 20°C staining with Alexa 488-conjugated anti-mouse IgG. CKRs are in green, whereas Tfn-R and CTx-B are in red. Images represent three experiments. (B) Cell surface distribution of receptors after detergent extraction. For visualizing CCR5, CD4, and Tfn-R in the same background, HeLa cells were transfected with CCR5 and CD4. CXCR4 was visualized in a HeLa CD4 clone expressing high levels of CXCR4. The two different protocols are described as in MATERIALS AND METHODS. CCR5 transfectants were stained with a mixture of CD4-FITC, 3A9-APC, and CD71-APC to visualize CD4, CCR5, and Tfn-R, respectively. CXCR4 was visualized using APC-conjugated 12G5 mAb. Single-channel images from two experiments are shown.

shown in Figure 9Aa, hardly any receptor antibodies were visualized on untreated cells. After prolonged agonist treatment (200 nM RANTES, 90 min), CCR5 was internalized to vesicles many of which colocalized with endogenous caveolin. By contrast, CXCR4 was endocytosed into vesicles that displayed little if any colocalization with caveolin-positive structures.

Next, we inquired whether trafficking of agonist-occupied CCR5 was altered by overexpression of caveolin-1 or caveolin-3 isoforms. Caveolin-1 was expressed as a GFP fusion protein (Cav1-GFP) that has been shown to preserve the subcellular distribution and function of endogenous caveolin-1 (Volonte *et al.*, 1999; Mundy *et al.*, 2002). As illustrated by Figure 9Ab, CCR5 underwent significant endocytosis

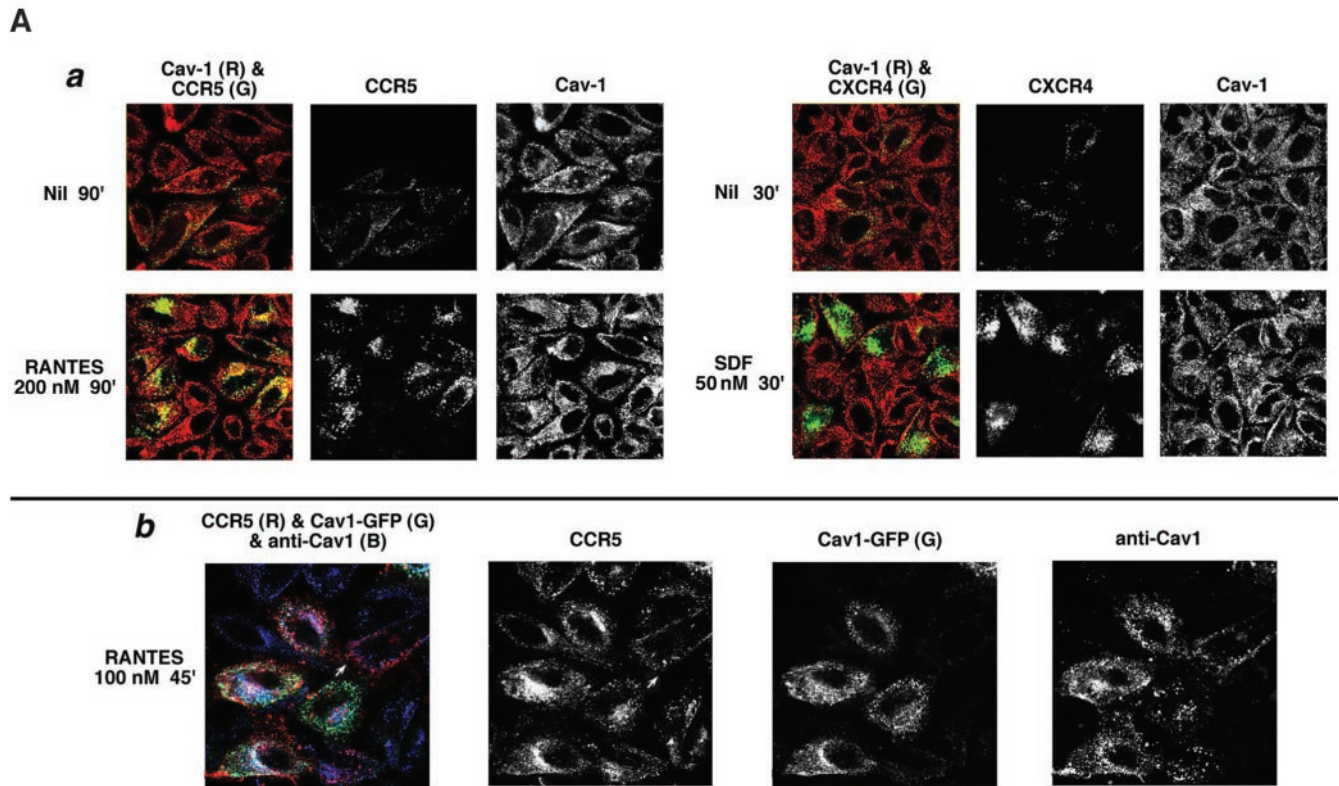


Figure 9.

after limited agonist treatment (100 nM RANTES, 45 min) in Cav1-GFP expressing cells, whereas in Cav1-GFP-negative cells (denoted by white arrows), most of the cell surface-bound antibody was not internalized and was stripped by acid-wash.

We also examined the trafficking pattern of CCR5 in HeLa cells expressing caveolin-3. To compare the receptor distribution (visualized by antibody feeding) between ligand-treated and untreated cells, cell surface-bound antibody was not stripped by acid-wash. In the absence of agonist, CCR5 was present predominantly at the cell surface (Figure 9Ba, left column). CCR5 trafficking was analyzed after limited ligand treatment (100 nM MIP-1 β , 30 min) that normally does not mobilize the receptor from the plasma membrane. In MIP-1 β -treated cells, CCR5 was internalized colocalizing in caveolin (colored red)-positive structures (Figure 9Ba). In caveolin-3 negative cells, CCR5 was predominantly on the surface after agonist treatment (denoted by arrows). The cell surface distribution of CCR5 in caveolin-3 nonexpressers that underwent limited agonist treatment was uniform. By contrast, in caveolin-3 expressers that were not treated with ligand, cell surface CCR5 exhibited a punctate and patchy distribution (image on the left). Caveolin-3 expression did not alter the clathrin-dependent trafficking pattern of ligand occupied CXCR4, KRFX-CCR5 mutant or Tfn-R (unpublished data). Because intracellular cholesterol transport is regulated by caveolin, we examined the cholesterol distribution in caveolin-expressing cells. Caveolin-3 positive cells

displayed reduced steady state levels of cholesterol at the plasma membrane, particularly cholesterol in the caveolin-positive regions of the cell surface (Figure 9Bb, NONE). Cholesterol repletion failed to repopulate these cholesterol-deficient domains (Figure 9Bb, CHLST).

Selective local loss of plasma membrane cholesterol seen in caveolin-positive cells may destabilize raft architecture, thereby allowing access of raft-anchored receptors to the clathrin pathway. We inquired whether inhibition of CCV formation affected the trafficking pattern of CCR5 in the context of caveolin expression. HeLa cells were cotransfected with GFP-tagged E Δ 95/295 mutant, caveolin-3 and CCR5. Agonist-mediated CCR5 trafficking was examined in an antibody feeding experiment as above except that cell surface-bound antibody was stripped by acid wash. In untreated cells, CCR5 was not internalized and most cell surface-bound antibody was removed by acid wash (Figure 9Bc). In cells not expressing E Δ 95/295, agonist-occupied CCR5 was internalized with substantial colocalization with caveolin-3 (denoted by arrows in Figure 9Bc). In cells expressing both caveolin and E Δ 95/295, agonist-treated CCR5 underwent internalization and colocalized within distinct caveolin-positive structures as shown in Figure 9Ba. From these findings, we concluded that caveolin-3-induced depletion of plasma membrane cholesterol did not significantly route agonist-occupied CCR5 to a clathrin-dependent itinerary.

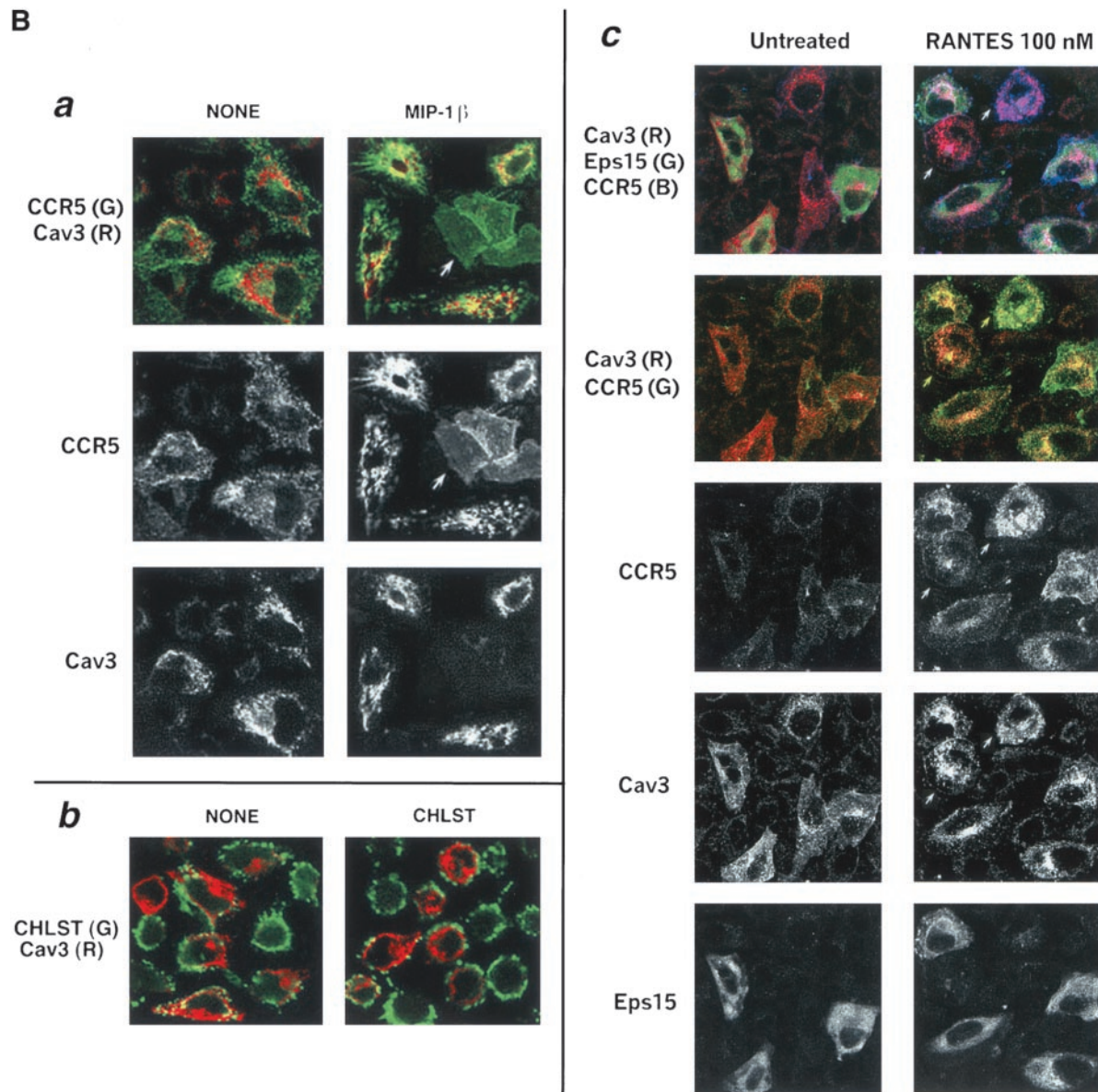


Figure 9 (continued from facing page). (A) Caveolin-1 and -3 differentially regulate agonist-dependent endocytosis of CCR5 and CXCR4. HeLa cells were transfected with the indicated chemokine receptor and treated with the indicated agonists. Cell surface-bound antibody was stripped by acid wash. Color overlays and individual channels are laid out left to right. R, red; G, green; B, blue. (a) Endocytic trafficking patterns of agonist-occupied CCR5 and CXCR4 in HeLa cells transfected for endogenous caveolin-1. Receptor endocytosis was visualized by antibody feeding using APC-conjugated 1° mAbs (pseudocolored green). Caveolin-1 was detected by staining with rabbit anticaveolin-1 IgG followed by 2° staining with Alexa 488-conjugated anti-rabbit IgG (red). (b) CCR5 trafficking in HeLa cells overexpressing caveolin-1-GFP. Agonist treatment was restricted to 45 min at 100 nM to limit CCR5 endocytosis. CCR5 trafficking was visualized by feeding unconjugated 3A9 mAb. Internalized antibody was visualized by staining with Alexa 568-conjugated anti-mouse IgG. Fluorescence from exogenous Cav1-GFP is in green. Both endogenous and plasmid-expressed caveolin-1 were detected by staining with rabbit IgG against caveolin-1 followed by staining with Alexa 647-labeled anti-rabbit IgG as the 2° reagent. Note that Cav1-GFP fluorescence and Cav1 antibody staining do not overlap completely, presumably because the epitope recognized by rabbit antibody is not exposed on all caveolin molecules. (B) Overexpression of caveolin-3 (Cav3). Agonist-treated CCR5 is internalized into caveolin-positive vesicles by largely clathrin-independent pathways, and these cells display selective depletion of plasma membrane cholesterol. Antibody feeding with APC-conjugated 3A9 mAbs monitored the trafficking of CCR5 induced by the indicated agonists at 100 nM for 30 min. HA-tagged Cav-3 (Cav3) was detected by staining with biotin-conjugated anti-HA mAb, followed by Alexa 488- (a) or TR- (c) labeled neutravidin. Images reflect results of three experiments. R, red; G, green; B, blue. (a) Composite images of CCR5 (green) and Cav3 (red) are shown at the top, with the monochromatic images of CCR5 and Cav3 below. (b) Staining for cell surface cholesterol in Cav3 transfectants. Cells were fixed and stained for cholesterol (CHLST, green) by filipin (10 μ g/ml) and then permeabilized and stained for Cav3 (red). (c) Eps15 mutant does not eliminate Cav3-enhanced endocytosis of ligand-occupied CCR5. HeLa cells were cotransfected with HA-tagged Cav3 (Cav3), GFP-tagged mutant E Δ 95/295 of Eps15 (Eps15), and CCR5. Receptor endocytosis assay was as above except that cell surface-bound antibody was stripped by acid wash. Trichromatic, bichromatic, and monochromatic images are displayed from top to bottom.

DISCUSSION

We have demonstrated that agonist-induced endocytosis of the chemokine receptor/HIV coreceptor CCR5 is 5–10-fold slower than that of CXCR4 in primary T cells and expression systems. We found that the molecular basis for the difference in endocytic rates lies in the C-terminal cytoplasmic domain, which anchored CCR5 in plasma membrane rafts, whereas CXCR4 was excluded from rafts. Further, we found that internalization of agonist-occupied CXCR4 proceeded primarily via a clathrin-dependent pathway, whereas CCR5 endocytosis was clathrin independent.

The kinetics of chemokine-induced internalization of CCR5 and CXCR4 may affect at least two distinct biological processes: leukocyte trafficking and HIV infection. With regard to leukocyte trafficking, receptor internalization is thought to be the mechanism by which cells become ultimately desensitized to persistent stimulation with chemokines. Receptors with large differences in their susceptibility to desensitization might be expected to have important differences in biological function. CCR5 has defined roles in inflammation, host response to infection, and autoimmunity (Locati and Murphy, 1999), whereas CXCR4 is a homeostatic receptor important in hematopoiesis, progenitor cell trafficking, and in early developmental programs in the vascular and nervous systems (Murdoch, 2000). Ligand regulation and receptor distribution are very different for CCR5 and CXCR4, and these differences clearly account for some of the biological distinctions between these receptors; however, the rate of endocytosis may also be involved. For instance, WHIM's syndrome, a rare inherited disorder characterized by warts, hypogammaglobulinemia, immunodeficiency, and myelokathexis has been genetically linked to a mutation in CXCR4, which truncates the C-terminal domain of the receptor and decreases receptor desensitization and endocytosis (Diaz, G., personal communication). Similarly, the duration of the functional response was severely reduced for the nonpalmitoylated CCR5 mutant (Blanpain *et al.*, 2001), although this mutant was competent for chemokine binding and activation of Gai-mediated signaling pathway (Blanpain *et al.*, 2001; Kraft *et al.*, 2001; Percherancier *et al.*, 2001; Venkatesan *et al.*, 2001). This defect is consistent with the rapid trafficking that we have shown for this mutant.

With regard to HIV pathogenesis, internalization of HIV coreceptors such as CCR5 and CXCR4 has been proposed as a potentially important mechanism by which endogenous ligands for these receptors may modulate HIV replication and disease pathogenesis (Amara *et al.*, 1997; Simmons *et al.*, 1997; Brandt *et al.*, 2002; Si *et al.*, 2002). In this regard, it is interesting to note that these receptors do not play an equivalent role in HIV pathogenesis. CCR5-specific HIV strains transmit disease and are present throughout the course of illness, whereas CXCR4-specific strains are typically found in only a minority of patients and only in the terminal stages of disease (D'Souza and Harden, 1996). Although an explanation for this striking dichotomy is currently lacking, the relative resistance of CCR5 to internalization that we have shown might be relevant because this could stabilize the CCR5 target relative to that of CXCR4 and thereby provide a selective advantage for R5-tropic HIV.

Whereas our results for agonist-induced CXCR4 trafficking in human epithelial cells agree with earlier reports (Amara *et al.*, 1997; Signoret *et al.*, 1998), in the case of CCR5,

they differ. In transfected CHO cells (Mack *et al.*, 1998), similar rates of endocytosis were reported for CCR5 and CXCR4. However, a recent report showed that even in CHO cells CCR5 was internalized by clathrin- and caveolae-dependent pathways (Mueller *et al.*, 2002). In HEK293 and COS-7 cells, failure of agonist occupied CCR5 to become phosphorylated, desensitized, and sequestered has been presumed to reflect the relative deficiency of GRK and/or β -arrestin in these cell types (Aramori *et al.*, 1997). However, this is unlikely to be the sole explanation for several reasons. First, we have found that CCR5 was consistently internalized slowly compared with other chemokine receptors tested in the epithelial cell types tested. Second, in HEK293 and HeLa cells, CCR5 was readily phosphorylated and desensitized after agonist binding and these are GRK/ β -arrestin-dependent processes (Venkatesan *et al.*, 2001, 2002). Third, CCR5 internalization was also retarded in PBLs, which express both GRK and β -arrestin. Most importantly, in our model expression systems the two receptors faithfully mimic the endocytosis phenotype found in primary T cells, which makes this system relevant for detailed mechanistic studies.

Mutagenesis analysis showed that the C-terminal domain of CCR5 harbors critical determinants of internalization. First, when the C terminus of CCR5 was progressively shortened, a slight increase in the rate of receptor internalization was observed for a mutant ending at amino acid 324. Second, when the truncation was further extended to a cluster of cysteines, which prevents receptor palmitoylation, a marked increase in the rate of endocytosis was observed, approximating that of wild-type CXCR4 and Tfn-R. Third, the KRFX mutant that lacked the serines in the C-tail, which are the targets for GRK phosphorylation, was endocytosed upon agonist binding. This suggests that receptor phosphorylation is not a critical determinant of β -arrestin recruitment to the agonist-occupied CCR5. Alternatively, serine residues in the ICLs may be phosphorylated by GRKs and serve as β -arrestin recruitment sites, as has been shown previously for CXCR4 (Cheng *et al.*, 2000). Fourth, substituting the C-tail of CCR5 for the C-tail of CXCR4 transferred the slow trafficking phenotype of CCR5 to the X4-R5 chimera. We and others have previously shown that the C-terminal domain of CCR5, including the cysteine cluster is crucial for the anterograde transport of the receptor to the plasma membrane (Blanpain *et al.*, 2001; Kraft *et al.*, 2001; Percherancier *et al.*, 2001; Venkatesan *et al.*, 2001). Interestingly, the C tail of CCR5 did not affect the anterograde transport when tested in chimeric receptors (Venkatesan *et al.*, 2001). Thus the C-tail of CCR5 performs a dual role: 1) facilitation of plasma membrane insertion of CCR5 and 2) protracted residence of activated receptor at the plasma membrane.

We have made some progress in identifying the cellular factors that explain why CCR5 and CXCR4 internalize at different rates, particularly with regard to plasma membrane microdomains, clathrin, caveolin, and rab5, a critical regulator of early endosomal function (Somsel Rodman and Wandinger-Ness, 2000). Endocytosis of both agonist-occupied CCR5 and the X4-R5 chimera was slightly enhanced in cells expressing exogenous wt rab5, whereas in cells expressing the hyperactive rab5, there was considerable trapping of CCR5 in morphologically distinct endosomes, without quantitative transfer of the receptor from the plasma mem-

brane to the endosomes. Conversely, excess wt rab5 did not enhance the already robust endocytosis of CXCR4. Genetic inhibition of rab5 function (Stenmark *et al.*, 1994) caused coordinate loss of endocytic transport of CXCR4 and Tfn-R, implying that these two receptors follow common pathways to early endosomes.

Genetic perturbation of clathrin assembly by a dominant negative Eps15 mutant (Chen *et al.*, 1998; Benmerah *et al.*, 1999) provided evidence for trafficking of CXCR4 via the clathrin pathway. In particular, in cells expressing the Eps15 mutant, there was coordinate inhibition of endocytosis of Tfn and CXCR4 receptors. By the above criteria, trafficking of CCR5-KRFX was judged to be also clathrin dependent. These conclusions were supported by kinetic analysis of agonist-occupied receptor transport to CCVs. CXCR4 and the KRFX mutant were transported to CCVs within 2–10 min of agonist binding, whereas a substantial fraction of CCR5 remained at the cell surface even after 20–40 min. However, a significant fraction of CCR5 endocytosis occurred in the presence of two different genetic inhibitors of CCV assembly, namely the Eps15 mutant (Benmerah *et al.*, 1999) and the C-terminal fragment of AP180 (Ford *et al.*, 2001), suggesting additional clathrin-independent itineraries for CCR5.

Proteins such as CCR5, which have saturated fatty acid chains that prefer an extended conformation, are able to partition into lipid rafts, the sphingolipid and cholesterol-rich plasma membrane microdomains that exist as discrete lateral assemblies (Melkonian *et al.*, 1999). Evidence that CCR5 is located in rafts included the observation that global extraction of cholesterol by cyclodextrin reduced the cell surface density of CCR5 and X4-R5, but not that of CCR5-KRFX or Tfn-R. The differential stability of cell surface receptors to cyclodextrin treatment must, however, be interpreted with caution. At higher levels than those used for extraction of plasma membrane CCR5, some other chemokine receptors (including CXCR4) and their derivatives could be extracted without affecting Tfn-R levels (our unpublished results). Endocytosis of residual plasma membrane CCR5 after cyclodextrin extraction was no better than that on untreated cells, and cyclodextrin treatment abolished signaling from CCR5. The residual cyclodextrin resistant fraction of CCR5 may not be fully palmitoylated and so not raft associated; it is also likely high levels of CCR5 expression in transfectants may exceed the “saturable” raft domains in the plasma membrane. These observations suggest that raft association may be a critical determinant for CCR5 function. In general, receptors that were readily extracted by cyclodextrin treatment resisted detergent solubilization. CCR5 and CD4 behaved in this manner. The KRFX mutant and Tfn-R were detergent sensitive. CXCR4 exhibited an intermediate sensitivity to detergent extraction. Copatching experiments further supported the predominant raft association of CCR5. CCR5, but not CXCR4, copatched with CTx-B, which clusters on the GM1 ganglioside in raft domains. X4-R5, which has the C-tail of CCR5, also copatched with this raft marker, whereas the KRFX mutant lacking the palmitoylation motif did not. Cyclodextrin effects suggested that CCR5 is probably raft-associated in primary leukocytes too. In particular, we found that this agent was fivefold more potent at reducing receptor expression on the cell surface and agonist responsiveness

for CCR5 than for CXCR4 in PBLs (our unpublished results).

Other groups have also investigated the association of CCR5 and CXCR4 with rafts, but no clear consensus has emerged. For instance, in HEK-293 cells, it was estimated that 11–18% of CCR5 was raft associated (Manes *et al.*, 1999). Although CXCR4 was largely excluded from rafts, HIV binding induced lateral migration of CXCR4 to raft domains (Manes *et al.*, 1999). A subsequent report showed that CXCR4 in PBLs and T cell lines was excluded from rafts irrespective of HIV binding (Kozak *et al.*, 1999). More recently it was shown that in T cell lines, both CCR5 and CXCR4, were raft associated and required cholesterol for optimal signaling (Nguyen and Taub, 2002a, 2002b) and productive HIV infection (Liao *et al.*, 2001; Popik *et al.*, 2002). Some of the above inconsistencies stem from the use of different cell types, and the various assays for raft association were not designed to analyze the cell surface receptors exclusively. By using three complementary assays, we have shown that cell surface CCR5 is raft associated and established the palmitoylated C-tail of CCR5 as the determinant of this phenotype. Raft-association of CXCR4 and other CKRs is debatable. We have shown that CXCR4 is not completely extracted by Triton X-100 at 4°C, and among the human CKRs, there is a hierarchy of raft-association (Venkatesan, S. *et al.*, unpublished data).

Given the preferential raft association of CCR5 and the apparent lack of a role for clathrin, what would be the alternative nonclathrin pathways followed by the agonist-bound receptor? Our data suggest a potential role for caveolae. These structures form by coalescence of detergent-resistant membrane microdomains (DRMs) and are stabilized by the cholesterol-binding protein caveolin. Although vesicular transport in endothelial cells has long been thought to proceed constitutively via caveolae, their role in leukocytes is not defined (Anderson, 1998). In our model system, CCR5 molecules internalized by agonist treatment appeared to colocalize in vesicular structures enriched in endogenous caveolin. Furthermore, in cells overexpressing muscle-specific caveolin-3 or the more ubiquitous caveolin-1, CCR5 but not CXCR4 was internalized into caveolin-positive structures. Enhanced trafficking of agonist-occupied CCR5 in caveolin-overexpressing cells correlated with a relative depletion of plasma membrane cholesterol. Cholesterol extraction and the resulting raft disruption may facilitate access of certain raft proteins to signaling, and the clathrin-dependent endocytic machinery as has been suggested for EGFR (Furchi and Anderson, 1998; Roepstorff *et al.*, 2002). Such was not the case for CCR5, as agonist-treated CCR5 was internalized to caveolin-enriched structures in cells coexpressing caveolin and the Eps15 mutant, which inhibits CCV formation.

Despite this suggestive evidence, it is important to note that our experiments have not directly addressed the role(s), if any of caveolae or caveolin in agonist-dependent trafficking of CCR5. Recent reports have shown that both DRMs and glycolipid rafts are able to undergo endocytosis in the absence of caveolin. One caveat in interpreting this is that caveolae could still represent a brief vesicular intermediate in such cells, and evidence from using budding inhibitors and caveolin overexpression indicates that this may be the case (Le *et al.*, 2002; Thomsen *et al.*, 2002; Le and Nabi, 2003).

Furthermore, caveolin-1 overexpression was shown to inhibit the clathrin-independent trafficking of autocrine motility factor receptor (AMF-R) and CTx-B to the ER and the Golgi, respectively (Le *et al.*, 2002; Le and Nabi, 2003). Unlike AMF-R that follows a direct route from the plasma membrane to the ER, CTx-B is delivered to the Golgi after a transit via the early endosomes.

In a recent study, caveolin overexpression selectively inhibited the ultimate delivery of CTxB to the Golgi but not the proximal transport of CTxB from the plasma membrane to the Tfn-R positive early endosomes (Le and Nabi, 2003). Other studies (Nichols *et al.*, 2001; Nichols, 2002) on the uptake of CTxB showed that it was endocytosed in a clathrin-independent manner to discrete caveolin-positive endosomes en route to the Golgi complex. Although CTxB colocalized with caveolin in all the intermediate organelles during its itinerary, caveolin itself was not transported to the Golgi. Also, the intracellular delivery of CTxB was not abolished when caveolin expression was severely inhibited by siRNA (Nichols, 2002), suggesting that caveolin was transported as a cargo rather than actively participating in the transport of CTxB. We have shown that the internalized CCR5 initially colocalized with caveolin-positive vesicles before being delivered to the early endosomes. In this regard, the endocytic itinerary of CCR5 is similar to the trafficking of the raft markers such as CTxB or GPI anchored GFP up to the Tfn-R-positive endosomal transit point. More experimental work is needed to resolve these issues.

The trafficking itinerary of CCR5 diverged from those of GPI-anchored proteins at a critical step. The endocytic delivery of GPI-anchored proteins to the Golgi complex was not blocked in cells expressing Rab5 S34N mutant, a known inhibitor of early endosomal function (Nichols *et al.*, 2001). By contrast, overexpression of wt or hyperactive rab5 caused endosomal stasis of CCR5, suggesting that early endosomes were a critical transit point in CCR5 trafficking. There is precedence for the delivery of raft-associated receptors to endosomes by different nonclathrin routes. For instance, the noncovalently assembled IL-2 receptor complex of α , β , and γ subunits is endocytosed by a nonclathrin pathway (Lamaze *et al.*, 2001) en route to a different destination for each subunit. All three subunits initially colocalize with Tfn-R-loaded endosomes. Whereas the β and γ chains are subsequently routed to rab7-positive late endosomes for degradation, the α chain is recycled back to the cell surface via recycling endosomes (Hemar *et al.*, 1995). CCR5 could be recycled in an analogous manner.

Future work will be needed to address the relevance of caveolae to endocytosis of CCR5 in lymphocytes. In this regard, we noted that CCR5 was internalized faster in activated PBLs than in resting cells (Figure 1). Resting lymphocytes lack detectable caveolae or caveolin, yet transport CTxB (Orlandi and Fishman, 1998). Endocytosis of agonist-occupied CCR5 probably follows a similar pathway. However, as suggested (Le *et al.*, 2002; Thomsen *et al.*, 2002), caveolae may exist in lymphocytes too, but may be rapidly converted into endocytic vesicles. It is possible that the enhanced CCR5 trafficking during immune cell activation is due in part to up regulation of caveolin (reviewed in Harris *et al.*, 2002), which may disrupt rafts. Alternatively, lipid remodeling, which occurs during immune cell activation and is known to redistribute several raft-embed-

ded receptors (Alonso and Millan, 2001; Sedwick and Altman, 2002), may facilitate agonist-mediated CCR5 internalization by clathrin-dependent or other noncoated vesicular transport.

Regardless of the trafficking itinerary of agonist-occupied CCR5, the prolonged transit time of stimulated receptor at the plasma membrane has important functional implications. A longer residence time of occupied receptors may permit ligand dissociation allowing resensitization before internalization. This may result in multiple rounds of G protein coupling from successive agonist binding events. The resulting local increment of $G\beta\gamma$ -dimers and β -arrestin may amplify cell signaling via the MAPK and other pathways facilitating cell movement and other responses.

The longer transit time of ligand-occupied CCR5 is also relevant to its usage as the coreceptor for M-tropic HIV infection. M-tropic infection of quiescent PBLs and monocytes is efficient despite low CCR5 density on the target CD4⁺ cells. In contrast, T-tropic infection of monocytes or macrophages requires high threshold levels of CXCR4 on the target cells (Tokunaga *et al.*, 2001). M- and T-tropic HIV gp120s function as agonists for CCR5 and CXCR4, respectively (Davis *et al.*, 1997; Weissman *et al.*, 1997). It is possible that M-tropic HIV gp41-mediated membrane fusion occurs efficiently during the long residence time of occupied CCR5 at the plasma membrane. Conversely, HIV *env* occupied CXCR4 may be rapidly internalized, potentially reducing the fraction of receptor for membrane fusion. This could provide a biochemical mechanism to explain why the transmitting strains of HIV are CCR5 tropic.

ACKNOWLEDGMENTS

We thank Ana Petrovic for technical assistance in preliminary experiments. We thank Jennifer Lippincott-Schwartz of NICHD, Eric Freed, Jonathan Silver, and Malcolm Martin of NIAID for discussion and comments. We acknowledge the contribution of several reagents by the NIH AIDS Research and Reference Reagent Program, Rockville, MD. R.L. was funded by a Canadian MRC postdoctoral fellowship.

REFERENCES

- Alkhatib, G., Locati, M., Kennedy, P.E., Murphy, P.M., and Berger, E.A. (1997). HIV-1 coreceptor activity of CCR5 and its inhibition by chemokines: independence from G protein signaling and importance of coreceptor downmodulation. *Virology* 234, 340–348.
- Alonso, M.A., and Millan, J. (2001). The role of lipid rafts in signaling and membrane trafficking in T lymphocytes. *J. Cell Sci.* 114, 3957–3965.
- Amara, A., Gall, S.L., Schwartz, O., Salamero, J., Montes, M., Loetscher, P., Baggiolini, M., Virelizier, J.L., and Arenzana-Seisdedos, F. (1997). HIV coreceptor downregulation as antiviral principle: SDF-1 α -dependent internalization of the chemokine receptor CXCR4 contributes to inhibition of HIV replication. *J. Exp. Med.* 186, 139–146.
- Anderson, R.G. (1998). The caveolae membrane system. *Annu. Rev. Biochem.* 67, 199–225.
- Aramori, I., Ferguson, S.S., Bieniasz, P.D., Zhang, J., Cullen, B., and Cullen, M.G. (1997). Molecular mechanism of desensitization of the chemokine receptor CCR-5, receptor signaling and internalization are dissociable from its role as an HIV-1 co-receptor. *EMBO J.* 16, 4606–4616.

- Benmerah, A., Bayrou, M., Cerf-Bensussan, N., and Dautry-Varsat, A. (1999). Inhibition of clathrin-coated pit assembly by an Eps15 mutant. *J. Cell Sci.* 112, 1303–1311.
- Berger, E.A., Murphy, P.M., and Farber, J.M. (1999). Chemokine receptors as HIV-1 coreceptors: roles in viral entry, tropism, and disease. *Annu. Rev. Immunol.* 17, 657–700.
- Berthiaume, L., and Resh, M.D. (1995). Biochemical characterization of a palmitoyl acyltransferase activity that palmitoylates myristoylated proteins. *J. Biol. Chem.* 270, 22399–22405.
- Blanpain, C. *et al.* (2001). Palmitoylation of CCR5 is critical for receptor trafficking and efficient activation of intracellular signaling pathways. *J. Biol. Chem.* 276, 2525–2530.
- Bleul, C.C., Farzan, M., Choe, H., Parolin, C., Clark-Lewis, I., Sordoski, J., and Springer, T.A. (1996). The lymphocyte chemoattractant SDF-1 is a ligand for LESTR/fusin and blocks HIV-1 entry. *Nature* 382, 829–833.
- Brandt, S.M., Mariani, R., Holland, A.U., Hope, T.J., and Landau, N.R. (2002). Association of chemokine-mediated block to HIV entry with coreceptor internalization. *J. Biol. Chem.* 277, 17291–17299.
- Brown, D.A., and London, E. (1998). Functions of lipid rafts in biological membranes. *Annu. Rev. Cell Dev. Biol.* 14, 111–136.
- Chen, H., Fre, S., Slepnev, V.I., Capua, M.R., Takei, K., Butler, M.H., Di Fiore, P.P., and De Camilli, P. (1998). Epsin is an EH-domain-binding protein implicated in clathrin-mediated endocytosis. *Nature* 394, 793–797.
- Cheng, Z.J., Zhao, J., Sun, Y., Hu, W., Wu, Y.L., Cen, B., Wu, G.X., and Pei, G. (2000). beta-Arrestin differentially regulates the chemokine receptor CXCR4-mediated signaling and receptor internalization, and this implicates multiple interaction sites between beta-arrestin and CXCR4. *J. Biol. Chem.* 275, 2479–2485.
- Cocchi, F., DeVico, A.L., Garzino-Demo, A., Arya, S.K., Gallo, R.C., and Lusso, P. (1995). Identification of RANTES, MIP-1 alpha, and MIP-1 beta as the major HIV-1 suppressive factors produced by CD8+ T cells. *Science* 270, 1811–1815.
- D'Souza, M.P., and Harden, V.A. (1996). Chemokines and HIV-1 second receptors. Confluence of two fields generates optimism in AIDS research. *Nat. Med.* 2, 1293–1300.
- Davis, C.B., Dikic, I., Unutmaz, D., Hill, C.M., Arthos, J., Siani, M.A., Thompson, D.A., Schlessinger, J., and Littman, D.R. (1997). Signal transduction due to HIV-1 envelope interactions with chemokine receptors CXCR4 or CCR5. *J. Exp. Med.* 186, 1793–1798.
- Ferguson, S.S., Zhang, J., Barak, L.S., and Caron, M.G. (1998). Molecular mechanisms of G protein-coupled receptor desensitization and resensitization. *Life Sci.* 62, 1561–1565.
- Ford, M.G., Pearce, B.M., Higgins, M.K., Vallis, Y., Owen, D.J., Gibson, A., Hopkins, C.R., Evans, P.R., and McMahon, H.T. (2001). Simultaneous binding of PtdIns(4,5)P2 and clathrin by AP180 in the nucleation of clathrin lattices on membranes. *Science* 291, 1051–1055.
- Furuchi, T., and Anderson, R.G. (1998). Cholesterol depletion of caveolae causes hyperactivation of extracellular signal-related kinase (ERK). *J. Biol. Chem.* 273, 21099–21104.
- Harder, T., Scheiffele, P., Verkade, P., and Simons, K. (1998). Lipid domain structure of the plasma membrane revealed by patching of membrane components. *J. Cell Biol.* 141, 929–942.
- Haribabu, B., Richardson, R.M., Fisher, I., Sozzani, S., Peiper, S.C., Horuk, R., Ali, H., and Snyderman, R. (1997). Regulation of human chemokine receptors CXCR4. Role of phosphorylation in desensitization and internalization. *J. Biol. Chem.* 272, 28726–28731.
- Harris, J., Werling, D., Hope, J.C., Taylor, G., and Howard, C.J. (2002). Caveolae and caveolin in immune cells: distribution and functions. *Trends Immunol.* 23, 158–164.
- Hemar, A., Subtil, A., Lieb, M., Morelon, E., Hellio, R., and Dautry-Varsat, A. (1995). Endocytosis of interleukin 2 receptors in human T lymphocytes: distinct intracellular localization and fate of the receptor alpha, beta, and gamma chains. *J. Cell Biol.* 129, 55–64.
- Keller, P., and Simons, K. (1998). Cholesterol is required for surface transport of influenza virus hemagglutinin. *J. Cell Biol.* 140, 1357–1367.
- Kozak, S.L., Kuhmann, S.E., Platt, E.J., and Kabat, D. (1999). Roles of CD4 and coreceptors in binding, endocytosis, and proteolysis of gp120 envelope glycoproteins derived from human immunodeficiency virus type 1. *J. Biol. Chem.* 274, 23499–23507.
- Kraft, K., Olbrich, H., Majoul, I., Mack, M., Proudfoot, A., and Oppermann, M. (2001). Characterization of sequence determinants within the carboxyl-terminal domain of chemokine receptor CCR5 that regulate signaling and receptor internalization. *J. Biol. Chem.* 276, 34408–34418.
- Krupnick, J.G., and Benovic, J.L. (1998). The role of receptor kinases and arrestins in G protein-coupled receptor regulation. *Annu. Rev. Pharmacol. Toxicol.* 38, 289–319.
- Krupnick, J.G., Goodman, O.B., Jr., Keen, J.H., and Benovic, J.L. (1997). Arrestin/clathrin interaction. Localization of the clathrin binding domain of nonvisual arrestins to the carboxy terminus. *J. Biol. Chem.* 272, 15011–15016.
- Kurzchalia, T.V., and Parton, R.G. (1999). Membrane microdomains and caveolae. *Curr. Opin. Cell Biol.* 11, 424–431.
- Lamaze, C., Dujeancourt, A., Baba, T., Lo, C.G., Benmerah, A., and Dautry-Varsat, A. (2001). Interleukin 2 receptors and detergent-resistant membrane domains define a clathrin-independent endocytic pathway. *Mol. Cell* 7, 661–671.
- Laporte, S.A., Oakley, R.H., Zhang, J., Holt, J.A., Ferguson, S.S., Caron, M.G., and Barak, L.S. (1999). The beta2-adrenergic receptor/betaarrestin complex recruits the clathrin adaptor AP-2 during endocytosis. *Proc. Natl. Acad. Sci. USA* 96, 3712–3717.
- Le, P.U., Guay, G., Altschuler, Y., and Nabi, I.R. (2002). Caveolin-1 is a negative regulator of caveolae-mediated endocytosis to the endoplasmic reticulum. *J. Biol. Chem.* 277, 3371–3379.
- Le, P.U., and Nabi, I.R. (2003). Distinct caveolae-mediated endocytic pathways target the Golgi apparatus and the endoplasmic reticulum. *J. Cell Sci.* 116, 1059–1071.
- Liao, Z., Cimasky, L.M., Hampton, R., Nguyen, D.H., and Hildreth, J.E. (2001). Lipid rafts and HIV pathogenesis: host membrane cholesterol is required for infection by HIV type 1. *AIDS Res. Hum. Retroviruses* 17, 1009–1019.
- Locati, M., and Murphy, P.M. (1999). Chemokines and chemokine receptors: biology and clinical relevance in inflammation and AIDS. *Annu. Rev. Med.* 50, 425–440.
- Mack, M. *et al.* (1998). Aminooxypentane-RANTES induces CCR5 internalization but inhibits recycling: a novel inhibitory mechanism of HIV infectivity. *J. Exp. Med.* 187, 1215–1224.
- Manes, S., Mira, E., Gomez-Mouton, C., Lacalle, R.A., Keller, P., Labrador, J.P., and Martinez, A.C. (1999). Membrane raft microdomains mediate front-rear polarity in migrating cells. *EMBO J.* 18, 6211–6220.
- Melkonian, K.A., Ostermeyer, A.G., Chen, J.Z., Roth, M.G., and Brown, D.A. (1999). Role of lipid modifications in targeting proteins to detergent-resistant membrane rafts. Many raft proteins are acylated, while few are prenylated. *J. Biol. Chem.* 274, 3910–3917.
- Mueller, A., Kelly, E., and Strange, P.G. (2002). Pathways for internalization and recycling of the chemokine receptor CCR5. *Blood* 99, 785–791.

- Mundy, D.I., Machleidt, T., Ying, Y.S., Anderson, R.G., and Bloom, G.S. (2002). Dual control of caveolar membrane traffic by microtubules and the actin cytoskeleton. *J. Cell Sci.* *115*, 4327–4339.
- Murdoch, C. (2000). CXCR 4, chemokine receptor extraordinaire. *Immunol. Rev.* *177*, 175–184.
- Murphy, P.M., Baggiolini, M., Charo, I.F., Hebert, C.A., Horuk, R., Matsushima, K., Miller, L.H., Oppenheim, J.J., and Power, C.A. (2000). International union of pharmacology. XXII. Nomenclature for chemokine receptors. *Pharmacol. Rev.* *52*, 145–176.
- Nguyen, D.H., and Taub, D. (2002a). Cholesterol is essential for macrophage inflammatory protein 1 beta binding and conformational integrity of CC chemokine receptor 5. *Blood* *99*, 4298–4306.
- Nguyen, D.H., and Taub, D. (2002b). CXCR4 function requires membrane cholesterol: implications for HIV infection. *J. Immunol.* *168*, 4121–4126.
- Nichols, B.J. (2002). A distinct class of endosome mediates clathrin-independent endocytosis to the Golgi complex. *Nat. Cell Biol.* *4*, 374–378.
- Nichols, B.J., Kenworthy, A.K., Polishchuk, R.S., Lodge, R., Roberts, T.H., Hirschberg, K., Phair, R.D., and Lippincott-Schwartz, J. (2001). Rapid cycling of lipid raft markers between the cell surface and Golgi complex. *J. Cell Biol.* *153*, 529–541.
- Nichols, B.J., and Lippincott-Schwartz, J. (2001). Endocytosis without clathrin coats. *Trends Cell Biol.* *11*, 406–412.
- Oberlin, E. *et al.* (1996). The CXCR4 chemokine SDF-1 is the ligand for LESTR/fusin and prevents infection by T-cell-line-adapted HIV-1. *Nature* *382*, 833–835.
- Orlandi, P.A., and Fishman, P.H. (1998). Filipin-dependent inhibition of cholera toxin: evidence for toxin internalization and activation through caveolae-like domains. *J. Cell Biol.* *141*, 905–915.
- Orsini, M.J., Parent, J.L., Mundell, S.J., and Benovic, J.L. (1999). Trafficking of the HIV coreceptor CXCR4. Role of arrestins and identification of residues in the c-terminal tail that mediate receptor internalization. *J. Biol. Chem.* *274*, 31076–31086.
- Percherancier, Y., Planchenault, T., Valenzuela-Fernandez, A., Virelizier, J.L., Arenzana-Seisdedos, F., and Bachelier, F. (2001). Palmitoylation-dependent control of degradation, life span, and membrane expression of the CCR5 receptor. *J. Biol. Chem.* *276*, 31936–31944.
- Popik, W., Alce, T.M., and Au, W.C. (2002). Human immunodeficiency virus type 1 uses lipid raft-colocalized CD4 and chemokine receptors for productive entry into CD4(+) T cells. *J. Virol.* *76*, 4709–4722.
- Radhakrishna, H., and Donaldson, J.G. (1997). ADP-ribosylation factor 6 regulates a novel plasma membrane recycling pathway. *J. Cell Biol.* *139*, 49–61.
- Roepstorff, K., Thomsen, P., Sandvig, K., and van Deurs, B. (2002). Sequestration of epidermal growth factor receptors in non-caveolar lipid rafts inhibits ligand binding. *J. Biol. Chem.* *277*, 18954–18960.
- Roy, S., Luetterforst, R., Harding, A., Apolloni, A., Etheridge, M., Stang, E., Rolls, B., Hancock, J.F., and Parton, R.G. (1999). Dominant-negative caveolin inhibits H-Ras function by disrupting cholesterol-rich plasma membrane domains. *Nat. Cell Biol.* *1*, 98–105.
- Sallusto, F., Mackay, C.R., and Lanzavecchia, A. (2000). The role of chemokine receptors in primary, effector, and memory immune responses. *Annu. Rev. Immunol.* *18*, 593–620.
- Scheiffele, P., Roth, M.G., and Simons, K. (1997). Interaction of influenza virus haemagglutinin with sphingolipid-cholesterol membrane domains via its transmembrane domain. *EMBO J.* *16*, 5501–5508.
- Schmid, S.L. (1997). Clathrin-coated vesicle formation and protein sorting: an integrated process. *Annu. Rev. Biochem.* *66*, 511–548.
- Sedwick, C.E., and Altman, A. (2002). Ordered just so: lipid rafts and lymphocyte function. *Sci STKE.* *122*, RE2.
- Si, Q., Kim, M., Zhao, M., Landau, N., Goldstein, H., and Lee, S. (2002). Vpr- and Nef-dependent induction of RANTES/CCL5 in microglial cells. *Virology* *301*, 342.
- Signoret, N., Rosenkilde, M.M., Klasse, P.J., Schwartz, T.W., Malim, M.H., Hoxie, J.A., and Marsh, M. (1998). Differential regulation of CXCR4 and CCR5 endocytosis. *J. Cell Sci.* *111*, 2819–2830.
- Simmons, G., Clapham, P.R., Picard, L., Offord, R.E., Rosenkilde, M.M., Schwartz, T.W., Buser, R., Wells, T.N.C., and Proudfoot, A.E. (1997). Potent inhibition of HIV-1 infectivity in macrophages and lymphocytes by a novel CCR5 antagonist. *Science* *276*, 276–279.
- Simons, K., and Ikonen, E. (1997). Functional rafts in cell membranes. *Nature* *387*, 569–572.
- Simons, K., and Ikonen, E. (2000). How cells handle cholesterol. *Science* *290*, 1721–1726.
- Simons, K., and Toomre, D. (2000). Lipid rafts and signal transduction. *Nat. Rev. Mol. Cell Biol.* *1*, 31–39.
- Somsel Rodman, J., and Wandinger-Ness, A. (2000). Rab GTPases coordinate endocytosis. *J. Cell Sci.* *113*(Pt 2), 183–192.
- Stenmark, H., Aasland, R., Toh, B.H., and D'Arrigo, A. (1996). Endosomal localization of the autoantigen EEA1 is mediated by a zinc-binding FYVE finger. *J. Biol. Chem.* *271*, 24048–24054.
- Stenmark, H., Parton, R.G., Steele-Mortimer, O., Lutcke, A., Gruenberg, J., and Zerial, M. (1994). Inhibition of rab5 GTPase activity stimulates membrane fusion in endocytosis. *EMBO J.* *13*, 1287–1296.
- Sugita, M., Grant, E.P., van Donselaar, E., Hsu, V.W., Rogers, R.A., Peters, P.J., and Brenner, M.B. (1999). Separate pathways for antigen presentation by CD1 molecules. *Immunity* *11*, 743–752.
- Thomsen, P., Roepstorff, K., Stahlhut, M., and van Deurs, B. (2002). Caveolae are highly immobile plasma membrane microdomains, which are not involved in constitutive endocytic trafficking. *Mol. Biol. Cell* *13*, 238–250.
- Tokunaga, K., Greenberg, M.L., Morse, M.A., Cumming, R.I., Lyerly, H.K., and Cullen, B.R. (2001). Molecular basis for cell tropism of CXCR4-dependent human immunodeficiency virus type 1 isolates. *J. Virol.* *75*, 6776–6785.
- Venkatesan, S., Petrovic, A., Locati, M., Kim, Y.O., Weissman, D., and Murphy, P.M. (2001). A membrane-proximal basic domain and cysteine cluster in the C-terminal tail of CCR5 constitute a bipartite motif critical for cell surface expression. *J. Biol. Chem.* *276*, 40133–40145.
- Venkatesan, S., Petrovic, A., Van Ryk, D.I., Locati, M., Weissman, D., and Murphy, P.M. (2002). Reduced cell surface expression of CCR5 in CCR5Delta 32 heterozygotes is mediated by gene dosage, rather than by receptor sequestration. *J. Biol. Chem.* *277*, 2287–2301.
- Volonte, D., Galbiati, F., and Lisanti, M.P. (1999). Visualization of caveolin-1, a caveolar marker protein, in living cells using green fluorescent protein (GFP) chimeras. The subcellular distribution of caveolin-1 is modulated by cell-cell contact. *FEBS Lett.* *445*, 431–439.
- Weissman, D., Rabin, R.L., Arthos, J., Rubbert, A., Dybul, M., Swoford, R., Venkatesan, S., Farber, J.M., and Fauci, A.S. (1997). Macrophage-tropic HIV and SIV envelope proteins induce a signal through the CCR5 chemokine receptor. *Nature* *389*, 981–985.